



HAL
open science

Nd(III) sorption using aminophosphonate-based sorbents – Sorption properties and application to the treatment of REE concentrate

Enas Imam, Ahmed Hashem, Xingmei Lu, Ahmad Tolba, Mohammad Mahfouz, Jiayu Xin, Ibrahim El-Tantawy El-Sayed, Said Mohamady, Abdullah A.S. Ahmed, Ahmed Galhoum, et al.

► To cite this version:

Enas Imam, Ahmed Hashem, Xingmei Lu, Ahmad Tolba, Mohammad Mahfouz, et al.. Nd(III) sorption using aminophosphonate-based sorbents – Sorption properties and application to the treatment of REE concentrate. *Colloids and Surfaces A: Physicochemical and Engineering Aspects*, 2024, 685, pp.133339. 10.1016/j.colsurfa.2024.133339 . hal-04459210

HAL Id: hal-04459210

<https://imt-mines-ales.hal.science/hal-04459210v1>

Submitted on 15 Feb 2024

HAL is a multi-disciplinary open access archive for the deposit and dissemination of scientific research documents, whether they are published or not. The documents may come from teaching and research institutions in France or abroad, or from public or private research centers.

L'archive ouverte pluridisciplinaire **HAL**, est destinée au dépôt et à la diffusion de documents scientifiques de niveau recherche, publiés ou non, émanant des établissements d'enseignement et de recherche français ou étrangers, des laboratoires publics ou privés.

Nd(III) sorption using aminophosphonate-based sorbents – Sorption properties and application to the treatment of REE concentrate

Enas A. Imam^a, Ahmed I. Hashem^b, Xingmei Lu^{c,d,e,*}, Ahmad A. Tolba^a, Mohammad G. Mahfouz^a, Jiayu Xin^{c,e}, Ibrahim El-Tantawy El-Sayed^{f,**}, Said I. Mohamady^a, Abdullah A. S. Ahmed^f, Ahmed A. Galhoum^{a,**}, Eric Guibal^g

^a Nuclear Materials Authority, P.O. Box 530, El-Maadi, Cairo, Egypt

^b Chemistry Department, Faculty of Science, Ain Shams University, Abassia, Cairo, Egypt

^c Beijing Key Laboratory of Ionic Liquids Clean Process, CAS Key Laboratory of Green Process and Engineering, State Key Laboratory of Multiphase Complex Systems, Innovation Academy for Green Manufacture, Institute of Process Engineering, Chinese Academy of Sciences, Beijing 100190, China

^d School of Chemistry and Chemical Engineering, University of Chinese Academy of Sciences, 100049 Beijing, China

^e Sino Danish College, University of Chinese Academy of Sciences, Beijing 100049, China

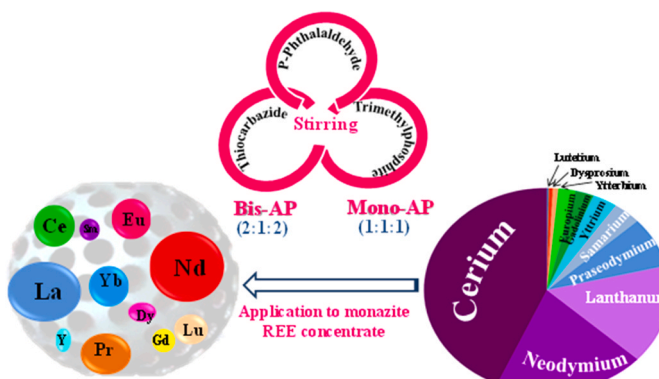
^f Chemistry Department, Faculty of Science, Menoufia University, Shebin El-Kom, Egypt

^g Polymers Composites and Hybrids (PCH), IMT Mines Ales, Ales, France

HIGHLIGHTS

- Simple one-pot synthesis of aminophosphonate-based sorbents for Nd(III) sorption.
- At pH 4.5, maximum sorption capacity reaches 1.28-1.40 mmol Nd g⁻¹.
- Sorption is exothermic and spontaneous, isotherms fitted by Sips equation while
- Equilibrium reached in 60 min; kinetics fitted by pseudo-first order rate equation.
- Preference for Nd and La among rare earth elements (in pre-treated ore leachate).

GRAPHICAL ABSTRACT



Keywords:

Neodymium & rare earth elements
Aminophosphonates
XPS
Uptake kinetics & sorption isotherms
Desorption
Thermodynamics

ABSTRACT

The rare earth elements (REEs) recovery of becomes a strategic issue due to intense use in high-tech industry. One of the most important challenge in the valorization of minerals or waste resources concerns the REEs separation from heavy metals as well as their proper separation within the REEs' family. Two aminophosphates (AP) derivatives were previously prepared for uranium recovery from wastes by one-pot reaction of *p*-phthalaldehyde, trimethylphosphite and thiocarbazine (in different proportions, leading to Mono-AP and Bis-AP

* Corresponding author at: Beijing Key Laboratory of Ionic Liquids Clean Process, CAS Key Laboratory of Green Process and Engineering, State Key Laboratory of Multiphase Complex Systems, Innovation Academy for Green Manufacture, Institute of Process Engineering, Chinese Academy of Sciences, Beijing 100190, China.

** Corresponding authors.

E-mail addresses: xmlu@ipe.ac.cn (X. Lu), ibrahimtantawy@yahoo.co.uk (I.E.-T. El-Sayed), Galhoum_nma@yahoo.com (A.A. Galhoum).

sorbents). Herein, these sorbents are successfully tested for sorption of Nd(III). For Mono-AP and Bis-AP, the maximal sorption capacity reaches 1.3 and 1.4 mmol Nd g⁻¹, respectively at optimum pH (i.e., 4.5). The functionalization grade weakly affects sorption property at equilibrium (equilibrium is attained in 120–180 min). Uptake kinetics is described by PFORE. Sorption isotherms are fitted by the Sips equation. Neodymium sorption is exothermic and spontaneous, the entropy change remains below 6 J mol⁻¹ K⁻¹ (being higher for Bis-AP). Metal desorption is successfully operated with HCl (0.2 M) solutions and at the sixth cycle, the reduction in sorption and desorption efficiencies do not exceed 7% and 4%. The materials are tested for the REEs recovery of from pre-treated acid leachate of monazite concentrate. In this work which focuses on the REEs recovery, the sorbents show first a marked (unexpected, in terms of physicochemical characteristics) preference for Nd, but also (to a lesser extent) for La>Ce>Pr (i.e., heavy REEs). The mechanisms involved in Nd(III) sorption (investigated utilizing XPS and FTIR analyses) affirm the cross contributions of phosphonate moieties, amine groups (and to a lesser extent thiocarbonyl) with differences between Mono-AP and Bis-AP in terms of relative contributions.

1. Introduction

The increasing industrial global need in industry for REEs (rare earth elements) is directly associated with the strong development of high-tech devices and applications that incorporate these strategic metals: electronic devices, photovoltaic panels, super-magnets, catalysts, special ceramics, metallurgy and nuclear industry [1,2]. Playing with the gap between supply and demand recently became a geopolitical and economical threat in the frame of world globalization. At national and regional levels, strong incentives have been promulgated for developing strategic and ambitious politics for valorization of wastes and recycling of spent devices and materials. For example, the directives from European Commission addressed the problem of WEEE (waste electronic and electric equipment) [3], which may have substantial proportions of noble and valuable metals, and REEs [4,5]. Another incentive for creating procedures for metal ions recovery from industrial wastes (both solids, sub-products, or water flow) is associated with their toxicity and their strong impacts on human and living beings. More strict regulations are being established regarding the release of pollutants into the environment [6]. These environmental and strategic constraints may explain that numerous studies have been documented for the last decades on the development of new processes for REEs recovery from solid wastes and contaminated wastewater [7,8]. The challenge consists in turning waste products to valorizable materials [9–11].

In most cases, after physicochemical separation (using gravimetric, magnetic processes).

The transfer of REEs to the aqueous phase during the treatment of grinded solids (tailing, low-grade ores, wastes, etc.) requires a first step of leaching [12,13]. It is noteworthy that REEs in mineral deposits are frequently associated with radionuclides; their valorization from secondary mining resources requires separating valuable REEs from hazardous metals; this is another important challenge in this field [14]. Based on the composition of the leachates (kind of leaching agent, relative concentrations of target metals and competitor ions, etc.) different techniques can be used [15,16]: precipitation [14], solvent extraction ([17–20], relayed supported membranes [21,22] and impregnated resins systems [23]). Chelating resins [24–26], ion-exchange resins [27,28], or carbon-based sorbents [29,30] are frequently offering competitive solutions for the treatment of dilute solutions. The selectivity for target metals can be enhanced using ion-imprinted materials such as resins [31] or functionalized silica-based composite [32]. Over the past few decades, interest has also been maintained in alternative materials. Over the past few decades, interest has also been maintained in considering the use of bio-based materials: the weaker sorption properties may be compensated by cheaper costs [33].

Usually diluted solutions are preferentially processed using sorbents and resins (opposed to liquid extraction systems). These sorbent materials are frequently oriented by analogy with solvent extractants by grafting on synthetic or bio-based supports the active moieties (which showed good performance in solvent extraction system). Therefore, the functional groups the most frequently used incorporate sulfur (S as NR₂,

–S– groups, RSC(=O), –SH) [34,35], phosphorus (P as: P–OH groups and/or P = O) [36], oxygen (O in >C=O groups, –O–, –OH, –COOH) [37] and nitrogen (N as in >NH, –NH₂, –N = N–, C(=O)NH₂, –CN groups). In the case of mono-functional grafted derivatives, the increased content of reactive groups directly improves the sorption efficiency. When the grafted groups are different, the sorption efficiency enhancement may be accompanied by loss in selectivity for target metals: this is driven by (HABS) principles ([38,39]); complementary groups may attract other metal ions. However, the literature also showed that bifunctionality may also bring substantial synergistic effects through modulation of the accessibility to reactive groups [40], intraligand cooperation controlled by intraligand hydrogen bonding and hydrophilic behavior [41]. These modulations may contribute to enhanced sorption and improved selectivity. Hence, Dudarko et al. [42] demonstrated that the bi-functionalization of SBA-15 (mesostructured silica) using both phosphonic groups and EDTA significantly increased the adsorption capacity of rare earth elements (e.g., as Dy and Nd) and their separation from heavy metals.

Aminophosphonate compounds have been widely used in organo-catalysis and transition-metal catalysis [43,44], but also in solvent extraction of metal ions [45,46]. Logically, this high reactivity was adapted for the design of new resins and sorbents [47–49]. Hence, amino-phosphonate sorbents were studied for uranium recovery [25, 50–52]. The type of substituent on aminophosphonate moiety may influence the reactivity [53]. Hence, in the case of aminophosphonate produced using one pot procedure of salicylaldehyde, with diphenylphosphite and amine precursors, the triamine groups (from diethylenetriamine) are less favorable in terms of both sorption capacity and selectivity for lead recovery than using a diamine precursor (from ethylenediamine) [52]. Imam et al. [51] functionalized chitosan with α -aminophosphonate moieties bearing either methyl or phenyl groups for U(VI) sorption: methyl-derivative was more efficient (i.e., two times) due to the combination of proper inductive effect, steric hindrance and acid-base properties. The steric arrangement of reactive groups may also contribute to higher sorption capacity and/or enhanced selectivity.

Recently, a new sorbent has been synthesized by one-pot procedure of trimethylphosphite, *p*-phthalaldehyde, and thiocarbamide [54]. Changing the proportions of the three precursors (2:1:2 vs. 1:1:1) allowed synthesizing two sorbents Bis-AP and Mono-AP, respectively, that have various textural characteristics as well as variable contents of active groups (thiocarbonyl, phosphonate, and amine). While U(VI) sorption capacity was slightly increased with the bis-aminophosphonation (in conjunction with a depletion of mass transfer properties, due to depreciation of textural properties and steric hindrance), the major benefits were observed in terms of selectivity (with both synthetic solutions and ore leachate) and stability at recycling. Depending on the frequent presence of REEs in uranium-rich deposits, these two sorbents (herein called Bis-AP and Mono-AP, respectively, with synthesis yields as high as 84.8% and 88.9%, respectively) are investigated for the Nd(III) recovery. A brief reminder reports the main characteristics of the materials [54]; this is followed by an exhaustive study of the Nd(III) adsorption characteristics of Bis-AP

and Mono-AP from synthetic solutions, including pH effect, sorption isotherms, uptake kinetics, selectivity against competitor metals, recycling of sorbents and metal desorption (6 cycles). In the last part of the work, the sorption performances are also tested for the rare earth elements recovery from pre-treated monazite concentrate (with a special attention paid to the separation of REEs).

2. Materials and methods

2.1. Material synthesis

The synthesis of the materials was described in a previous study (including the materials and reagents used for their production) (Enas et al., 2023). The synthesis consists in a three component reaction (i.e., *p*-phthalaldehyde, trimethyl phosphite and thiocarbazine), with various molar ratios (i.e., 2:1:2 and 1:1:1) for producing Mono-AP and Bis-AP materials, respectively. The reaction took place in the presence of copper triflate (i.e., Cu(OTF)₂; Innochem, Beijing, China) as Lewis acid catalyst, in acetonitrile solvent, and for 72 h, at ambient temperature. By the end of the procedure, the materials had been air-dried (in addition to being kept within a desiccator till usage). The synthesis route and the sorbents structure are illustrated in [Scheme S1](#) (see [Supplementary Information](#), detailed procedure was previously described, [54]).

Neodymium solutions were prepared by dissolving of NdCl₃ (Sigma-Aldrich, Merck KGaA, Darmstadt, Germany) into 1 mL of concentrated (16.38 M) H₂SO₄ with heating followed by diluting to 1 g L⁻¹ (stock solution) in demineralized water. Prior to use, stock solution was diluted with demineralized water to provide metal solutions for sorption studies.

2.2. Characterization

The characterization of the sorbents was previously described [54] for the determination of morphology (by scanning electron microscopy) and particle size distribution (microscopy and image analysis), textural properties (BET analysis), crystallinity (X-ray diffraction), chemical content (elemental analysis, sand sample acid digestion followed by P spectrophotometric analysis using vanadate/molybdate procedure), pH_{PZC} (pH-drift titration method). Semi-quantitative EDX analysis was performed on Thermo Fisher Scientific model Prisma E with Color SEM Technology and integrated energy-dispersive X-ray spectroscopy was used for the acquirement of SEM images. Detailed analytical procedures and characterization results were previously described [54]. Specific complementary experiments were performed for characterizing the interaction modes between sorbents and Nd(III). A 4100 Jasco spectrophotometer (Jasco Corporation, Tokyo, Japan) was used to collect Fourier Transform infrared spectra, while X-ray photoelectron spectroscopy was performed on a Perkin Elmer PHI 5600 (Perkin Elmer Instruments, Waltham, MA, USA), with monochromatic X-ray Al K α radiation source (200 W energy) of samples deposited on indium sheets.

2.3. Sorption and desorption experiments

Sorption-desorption tests were performed in batch systems with agitation speed fixed to 200 rpm. Otherwise stated, 25 \pm 1 °C was the set temperature; otherwise stated (meaning for the thermodynamics study, where the sorption isotherms were collected at T: 35, 45, 55 \pm 1 °C). To prepare the solutions, the stock solution was diluted using distilled water; the pH was adjusted using sulfuric acid and sodium hydroxide solutions. The dose of the sorbent was maintained at 0.5 g L⁻¹ (S.D = m/V, wherein v is the soln. volume (L) and m is sorbent mass. During the pH factor investigation, the contact time was set at 120 min and C₀:035 mmol Nd L⁻¹ (initial metal ion concentration). For uptake kinetics, pH₀ (i.e., the initial pH) of the solution was fixed at 4.5. For sorption isotherms, the C₀ was ranged from 0 to 2.1 mmol Nd L⁻¹ (pH₀ 4.5 and contact time: 60 min). Throughout the sorption process, the pH was n

monitored, but the equilibrium pH (i.e., pH_{eq}) had been systematically measured (via a digital pH-meter of the type JENWAY 3310, within an error of \pm 0.01). In batch systems, desorption studies were also carried out with HCl (0.2 M) for metal desorption. The sorbent was abundantly rinsed by water after elution step (which took place in 60 min) before being re-used. Neodymium concentration in initial solution and collected samples (after filtration) was measured using ICP-AES analysis inductively-coupled plasma atomic emission spectrometry, Prism ICP, Teledyne Leeman, Labs. Hudson, NH, USA. To calculate the sorption capacity (q, mmol g⁻¹), the equation $q = (C_0 - C_{eq}) \times V/m$ (mass balance equation) was deduced.

To evaluate the desorption efficiency (DE, %), the amount eluted with HCl solution from Nd-loaded sorbent was compared to the amount initially sorbed). Sorption experiments are repeatedly carried out and the mean results are reported in the figures (with standard deviation). In the figure captions, the effective conditions of the experiments are briefly described.

For fitting experimental data of sorption isotherms and uptake kinetics, conventional equations were employed. [Table S1](#) (check out [Supplemental Information](#)) lists these equations: (a) Sips and Langmuir equations to fit the sorption isotherms and (b) PFORE and PSORE, and RIDE (Crank equation) to fit the uptake kinetics. Alternative equations (such as Dubinin-Radushkevich, Freundlich and Temkin equations) were also unsuccessfully applied to mode the isotherms (not shown). Akaike Information Criterion (AIC, [55]) and R² (determination coefficient) were used to monitor the fit efficiency.

2.4. Application to ore processing

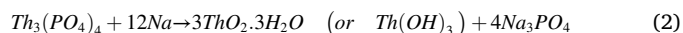
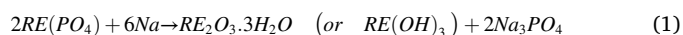
Sorbents were applied on monazite ore samples (alkaline leachates) from Abou-Kashaba, near Rosetta, Rashid City, Egypt, near Alexandria.

Egyptian monazite (purity: 97%) as an orthophosphate mineral linked to Th and REEs, is primarily composed of REOs (rare earth oxides), accounting for approximately 60% of the mineral's composition (which is mainly consisting of light REEs (LREEs): 26.55% (Ce₂O) and 34.35% (the other REE₂O₃), U₃O₈ (0.44%) and ThO₂ (5.9%).

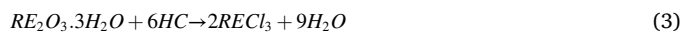
Alkaline leachates are typically chosen over acid leachates, essentially due to their cost competition and ease of control, although metal extraction from monazite may proceed either way.

Actually, a lower temperature is often needed for alkaline leaching than for acid treatment. Additionally, the byproducts (trisodium phosphate) may also be easily turned into fertiliser.

[56]. Schematizing the alkaline leaching in accordance with [Eqs. \(1–2\)](#) [57]:

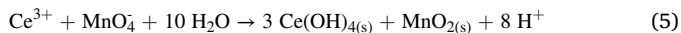


The alkali thermal treatment of monazite (by 50% NaOH (S/L: 1:1; time: 3 h; T: 140 °C in autoclave) produces a concentrated mix of hydrous/oxide cake (of REEs) that can be leached at 80 °C by hydrochloric acid solution, followed by dilution with water. Th and U cake can be isolated from REEs applying specific neutralization procedure at pH: 5.8–6 using an alkali (i.e. ammonia), while the REOs recovery can be achieved by raising the pH to 8.0–8.2 [57–59]). [Table S2](#) displays the chemical analysis of the REEs concentrate (in wt%). The REOs concentrate (1 g) was digested with 10 mL HCl (1 M) for 1 h at 80° to produce the rare earth pregnant liquor solution (PLS). Finally, the solution's volume was diluted to 200 mL. the schematization of the reactions can be provided by [Eqs. 3, 4](#):



The high Ce₂O₃ content may impact the sorption of Nd, hence Ce(III)

should be separated using previously reported separation technique [60]. Ce(III) is precipitated as Ce(IV) (ceric hydroxide (Ce(OH)₄) by combined oxidation and hydrolysis (using a mixture of 0.2 M KMnO₄ and 0.3 M Na₂CO₃). Cerium (III) oxidation can be schematized according to Eq. 5:



Cerium can be valorized by re-precipitation with Na₂CO₃ and calcination at 900 °C to yield ceric oxide (CeO₂). The residual neodymium concentration was reduced from 274.34 to 241.45 mg Nd L⁻¹; cerium precipitation caused partial loss of neodymium: to complete the sorption studies the leachate was diluted twice (to 400 mL) using demineralized water after processing Ce(III) precipitation; Nd concentration was diluted to 120.73 mg Nd g⁻¹. In the precipitated (diluted) pregnant liquor solution (PPLS), the supplementary loss of Nd(III) did not exceed 12%. Also, the cerium precipitation contributes to precipitating variable proportions of REEs (in the range 15.03% for Gd to 53.97% for Yb).

The sorption tests were performed in batch systems at selected conditions of: agitation speed: 200 rpm; T; 25 ± 1 °C; time: 60 min and pH₀: 3.8, the pH₀ was set to 3.8 to avoid REEs precipitation. After equilibrium, the solution was subjected to an ICP-AES analysis to determine the residual REE concentration after being filtered.

3. Result and discussion

3.1. Characterization of sorbents (and their interactions with Nd(III))

3.1.1. Reminder of physicochemical properties

Mono-AP and Bis-AP sorbents were previously characterized [51].

Table S3 summarizes these characteristics. The surface morphology of the developed raw sorbents particles was assessed using SEM (Fig. 1). Fig. 1a and b illustrate the surface morphology of both Mono-AP and Bis-AP sorbents, revealing a semi-spherical shape with some irregular particles and a compact structure with a relatively smooth surface. Moreover, the images suggest that the Bis-AP type is characterized by a slightly smaller average particle size (≈11.2 ± 5.7 μm) and a more regular spherical structure compared to Mono-AP (≈16.2 ± 8.6 μm), which shows a wider size dispersion. This is clearly indicated in the low-magnification images (Fig. 1a & b). However, following Nd(III) binding, a notable increase in surface roughness and compactness, along with visible interparticle spaces, was observed in the SEM image (Fig. 1c). This is particularly evident in the high-magnification image (Fig. 1c). This analysis was analyzed using SEM (Thermo Fisher Scientific model Prisma E with Color SEM Technology and integrated energy-dispersive X-ray spectroscopy was used for the acquirement of SEM images). The color images demonstrate the validation of Nd(III) loading through observable changes in the raw sorbents. Mono-AP (A) initially appears bright yellow, while Bis-AP (C) has a distinct fat color. After Nd(III) loading, both sorbents exhibit a noticeable shift to a nearly similar dark or slightly brown color, as depicted in (B) for Mono-AP and (D) for Bis-AP, as illustrated in Fig. 1 (the lower panel). The fully colored particles in (D), in-line with the experimental capacities and efficiencies.

In addition, the bi-functionalized material (little more crystalline) shows lower specific surface 58 vs. 95 m² g⁻¹ and pore volume associated with largest pore size (8.4 vs. 2.0 nm); meaning that the two sorbents can be ranked as mesoporous materials according IUPAC classification of pore size. The double grafting of aminophosphonate groups is confirmed by higher N and P contents, corresponding to suggested formula: C₁₁H₁₇N₄O₄PS and C₁₄H₂₈N₈O₆P₂S₂. The pH_{PZC} of the

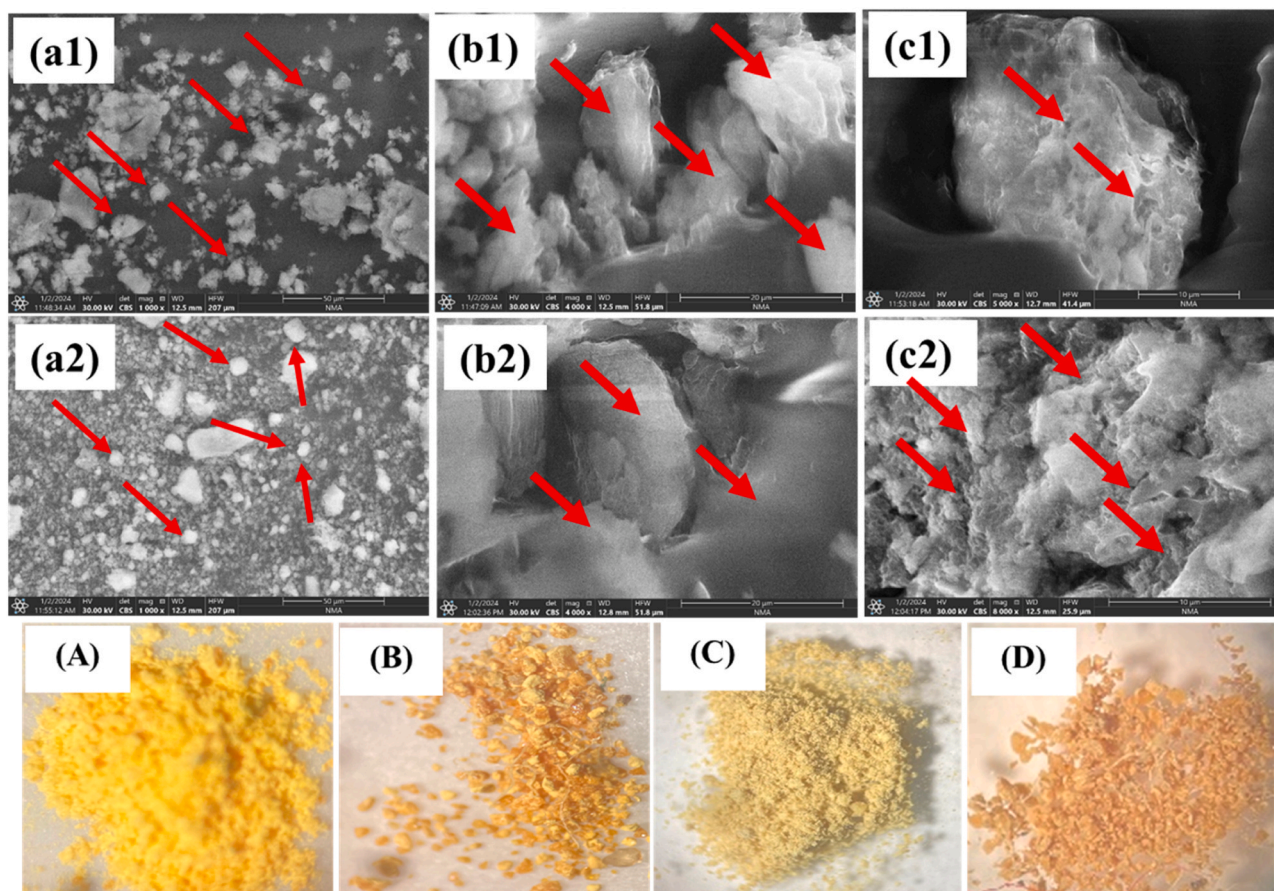


Fig. 1. SEM images analysis of Mono-AP (1), and Bis-AP (2) sorbents, before (a&b) and after Nd(III) sorption (c): at low magnification (at 1000 X (a)) and at high magnification (4000 X (b) and 5000 X (c)). The color images of raw sorbents (A) Mono-AP and (C) Bis-AP before, and after Nd(III) loading (B) and (D), respectively.

sorbents has slightly increased (from 5.5 to 6.1) as a result of these chemical changes, meaning that Bis-AP bears a positive global charge on a wider pH range.

3.1.2. FTIR analysis

Imam et al. [51] has already documented the interpretation of these FTIR spectra. Briefly, in the region $4000\text{--}2000\text{ cm}^{-1}$, the two sorbents showed similar FTIR profiles with broad bands, at around $3335\text{--}3227$ and $3188\text{--}3156\text{ cm}^{-1}$, that are attributed to -NH_2 as well as -NH vibration, respectively [53,61,62]. Vibrations associated with stretching of aromatic and aliphatic C-H groups were detected at $2981\text{--}2973\text{ cm}^{-1}$ and $2891\text{--}2850\text{ cm}^{-1}$, respectively ($\delta_{\text{C-H}}$ vibrations were also identified at $1418\text{--}1414$ and $1399\text{--}1381\text{ cm}^{-1}$, respectively; and out-of-plane $\delta_{\text{C-H}}$ vibration at $899\text{--}870\text{ cm}^{-1}$). -NH_2 as well as -NH groups were also detected at $1606\text{--}1594\text{ cm}^{-1}$, while $\nu_{\text{C-N}}$ was observed at $1506\text{--}1493\text{ cm}^{-1}$ and $\omega_{\text{N-H}}$ at $831\text{--}824\text{ cm}^{-1}$ [63–65]. Three sets of bands were detected; at $796\text{--}761\text{ cm}^{-1}$ (attributed to P-CH vibration), at $1073\text{--}1042\text{ cm}^{-1}$, $958\text{--}935\text{ cm}^{-1}$, $610\text{--}602\text{ cm}^{-1}$ (P-O-C symmetrical stretching) [66,67] and at $1264\text{--}1240\text{ cm}^{-1}$ for $\nu_{\text{P=O}}$ [51].

Additionally, the broad peak located at $1583\text{--}1519\text{ cm}^{-1}$ (specified to aromatic C=C bonds) and adsorption band detected at $1334\text{--}1315\text{ cm}^{-1}$ associated with the stretching vibration of C=S bonds [68], and the broad band located at $1583\text{--}1519\text{ cm}^{-1}$ (assigned to C=C bond, in aromatic rings) demonstrate the effective synthesis of the sorbents through the one pot reaction of thiocarbazide, trimethylphosphite, and *p*-phthalaldehyde. Hence, the FTIR spectra of Bis-AP and Mono-AP

(Fig. 2) include different functional groups (i.e., -C=S , P = O, -NH_2 and -NH-), which may be involved in the interactions with Nd(III).

Herein, the analysis is focused on the comparison of the sorbent's spectra at various steps of usage (Fig. 2): raw sorbent, after metal sorption, after sorption-desorption six cycles, after being conditioned at the sorption pH (pH_0 4.5) and after sorbent conditioning in HCl solute (0.3 M) the solution of metal desorption (sorbent elution solution). This sequence allows identifying the effective contribution of the interactions of the sorbent with the solute (independently of the variations caused by the changes in the environmental conditions of pH). Table S4 summarizes the assignments of FTIR bands; their comparison may help isolating the specific changes associated with metal binding. The Occurrence, delocalization, or evanescence of specific peaks and shifts in some peaks' relative intensities may all be related to these interactions [44]. The FTIR spectra of the sorbents are significantly changed by Nd(III) sorption: the increase in the intensities (at $3353\text{--}3227\text{ cm}^{-1}$) that belong to -NH_2 and -NH groups. The bands at 1602 cm^{-1} , 1604 cm^{-1} (associated with -NH_2 and >NH groups) are shifted to 1605 cm^{-1} and 1607 cm^{-1} . Also, the bands in the region: 1493 cm^{-1} as well as 1506 cm^{-1} associated with $\nu_{\text{C-N}}$ are shifted to 1496 cm^{-1} and 1509 cm^{-1} .

The vibrations of both Nd-N bond of C-N and Nd-N of N-H (of -NH_2 and >NH groups) caused these changes. After metal binding, the peaks at $796\text{--}761$, $958\text{--}935$ and $1264\text{--}1240\text{ cm}^{-1}$ specified with $\nu(\text{P-CH})$, $\nu(\text{P-O-C})$ and $\nu(\text{P=O})$ are delocalized (with simultaneous reduction in the intensity consistently with previous observations on U(VI) binding by aminophosphonate-based sorbents [53]). Nd(III) sorption has a negligible effect on the C=S peak at 1327 cm^{-1} ; the shifting $\sim 1\text{ cm}^{-1}$). It is noteworthy that in the Mono-AP sorbent, the peak at 1216 cm^{-1} related to aldehydic C-H group is delocalized to 1214 cm^{-1} where the peak at 1720 cm^{-1} corresponding to aldehydic C=O group is delocalized to 1714 cm^{-1} . FTIR spectra of the metal-loaded sorbents show delocalization, intensities reduction of the peaks that correspond to CHO-group (in Mono-AP sorbent) and phosphonate and amine groups (or at least alteration of their chemical surroundings) affirming the role of such functional groups in binding with Nd(III).

A new band at $637\text{--}620\text{ cm}^{-1}$ has been shown after neodymium sorption that can be correlated with the SO_4^{2-} anion [69]. The FTIR spectrum revealed many variations in comparative intensity for different bands at $600\text{--}800\text{ cm}^{-1}$ region, associated with N-Nd and (O-Nd-O) stretching [70]. The stability of the two sorbents after recycling has been confirmed by comparing the FTIR spectra following six cycles of adsorption and desorption.

The FTIR spectra of the sorbents (loaded with Neodymium) are only partly returned to their initial sorbents spectra after desorption (Fig. 2), with the peaks being moved but not entirely restoring to their initial wavenumbers. There are apparent shifts in amine group's bands at $1264\text{--}761\text{ cm}^{-1}$ and at the typical phosphonate peaks at $1264\text{--}761\text{ cm}^{-1}$. This implies that the amine and phosphonate groups are significantly affected by the sorbents regeneration.

3.1.3. XPS characterization

Before and after Nd(III) sorption, the sorbents' XPS spectra are shown in Fig. 3 with conventional N 1s (at Binding Energy, BE: $\sim 401\text{ eV}$), O 1s (BE: $\sim 533\text{ eV}$), C 1s (BE: $\sim 286\text{ eV}$), S 2s (BE: $\sim 227\text{--}230\text{ eV}$), P 2s (BE: $\sim 191\text{--}192\text{ eV}$), S 2p (BE: $\sim 163\text{--}166\text{ eV}$), and P 2p (BE: $\sim 133\text{--}134\text{ eV}$). After Nd(III) sorption, some shifts are observed and neodymium presence has been attested through the occurrence of the small peak associated with Nd 4d (BE: $\sim 124\text{--}127\text{ eV}$). This analysis is completed in Tables S5 and S6 by the comparison of high-resolution spectra for N1s, P 2p, O 1s, C 1s, S 2p, and Nd 3d_{5/2} for the two sorbents prior to and afterwards neodymium binding. This is completed by the table of assignments (BE values and atomic percentage) in Table S7.

The comparison of the XPS spectra shows roughly similar profiles between Mono-AP and Bis-AP for P 2p, N 1s, O 1s, C 1s, and, while the signal associated with S 2p is substantially different between the two sorbents; meaning that the bi-functionalization strongly affect the

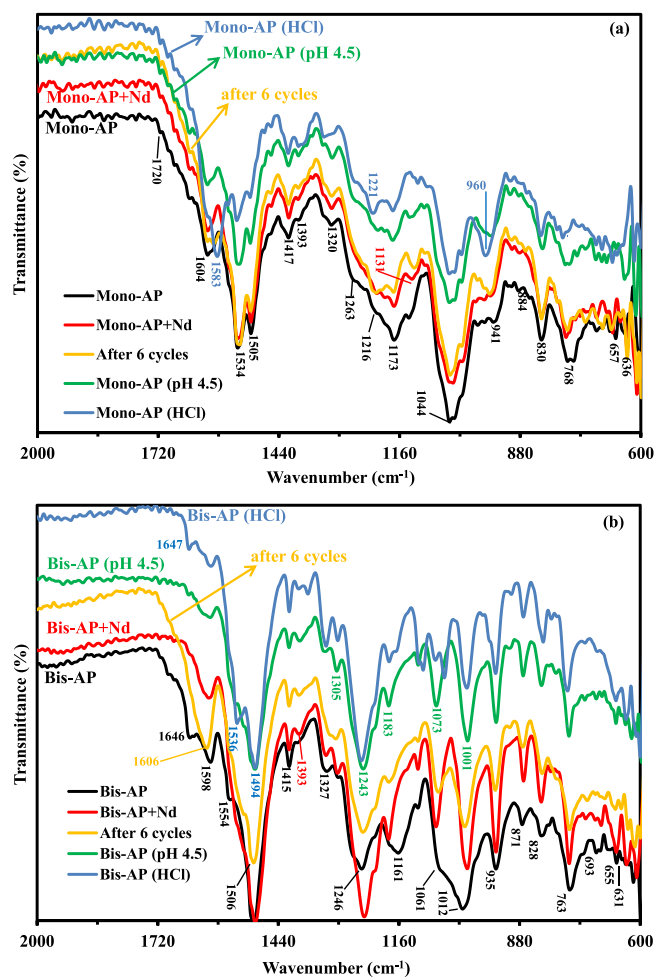


Fig. 2. FTIR spectra of Mono-AP (a) and Bis-AP (b) sorbents at different stages of use (raw, after conditioning at pH 4.5, after Nd(III) sorption at pH 4.5, after conditioning with HCl (similar to desorption test), and after 6 recycling steps).

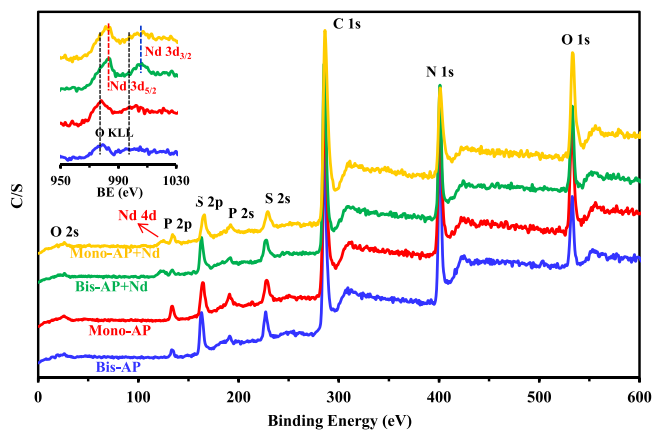


Fig. 3. XPS survey scans for Mono-AP (a) Bis-AP (b) sorbents before and after Nd(III) sorption.

environment of thiocarbonyl group. Minor changes are observed on the relative intensity of the bands around ~ 288 eV and ~ 286 eV and, meaning that the differential substitution of aminophosphonate affects the environment and the intensity of C-based groups (increase in the density of methyl and C-O-P groups and decrease of the AF of C-OH functions). The decrease of C-OH groups is affirmed by the evanescence of the peak at 534.8 eV for Bis-AP. The bis-functionalization decreases also the AF of C-N groups (at 403.0 eV (accompanied with a shift toward lower BE).

The Nd(III) adsorption on the sorbents is clearly demonstrated by the occurrence of a broad band in the range 988–968 eV (Nd $3d_{5/2}$ signal), where the signals' deconvolution reveals the existence of two bands appearing at ~ 983 eV and ~ 978 eV, which are associated with bonds of Nd(III) with N-based and O-based (in phosphonate units); the third component correspond to the superposition of Auger emission of O KLL band. It is noteworthy that the AFs for N-based and O-based bonds are hardly impacted with the sorbent nature (also, with the extent of aminophosphonation). In the case of Mono-AP, the main modifications are recognized for O 1 s signal (decrease of the peak at ~ 531 eV, compensated by the increase of the other signals), for C 1 s signal (enhancement of ~ 287 eV signal and occurrence of a new small band at ~ 291 eV), the N 1 s signal (increase of the peak at ~ 403 eV, shifted to ~ 402 eV and appearance of a small peak at ~ 405 eV). The S 2p signal is also characterized by an inversion between the two components after neodymium sorption. It is noteworthy that neodymium is present in the solution as a mixture of free metal and sulfate species (Nd^{3+} and NdSO_4^+ , respectively). The S 2p of sulfate species is expected to occur at higher BEs (such as ~ 169 eV); apparently sulfate anions are not appearing on the sorbent during neodymium sorption. Surprisingly, in the case of Bis-AP (despite little higher sorption than with Mono-AP) the differences in the core level spectra are less marked after metal sorption; the "global profiles" of the signals are weakly changed. The relative AF values have been recognized as the most substantial modifications.

The most significant changes are observed in terms relative AF values. For example, for C 1 s the variations for Bis-AP are reciprocal to those observed with Mono-AP (increase of 284.8 eV signal and decrease of 286 eV and 288 signals). For O 1 s, the trends are similar for the two sorbents. For N 1 s, the trends are also reversed between Mono-AP and Bis-AP, meaning probably a greater contribution of amine-based reactive groups; i.e., -N-H and -NH₂, because of higher density of amino functions). The signal P 2p (and its deconvoluted components) shows a greater relative contribution of O-P signal (associated to the active group in phosphonate). Reciprocally to Mono-AP, for Bis-AP the contribution associated with C-S-C is weakly reduced to increased proportion of S=C group.

From these changes, it appears that neodymium (as free trivalent Nd

(III) cation) is bound through interactions with amine groups (-NH and/or -NH₂), O-based groups (as phosphonate moieties). The contribution of thiocarbonyl groups cannot be neglected (weak effect on BEs and AFs). The differences observed in core-level spectra between Mono-AP and Bis-AP (especially inversions in the effect of metal sorption between the components) show that the relative contribution of the different mechanisms in Nd(III) sorption changes with the functionalization.

3.2. Nd(III) Sorption properties (synthetic solutions)

3.2.1. pH effect

With the double-grafting of aminophosphonate moieties the sorbent's pH_{PZC} is slightly switched to greater value (from 5.5 to 6.1); this means that the overall sorbent charge remains protonated over a broader pH spectrum. The overall charge reaches a maximum around pH 4. This active protonation groups may influence how metal binding is affected by pH since the positive charge induces repulsion effects against metal cations. Obviously, the metal ion speciation may also be influenced by the pH, which can then modulate the effect of surface charge of the sorbent. For Nd(III) (under preparation conditions of the solutions, at initial Nd(III) concentration: 0.35 mmol L^{-1}), Fig. S1 shows that cationic species hugely control all pH range: higher than pH 3, anionic species (as $\text{Nd}(\text{SO}_4)_2^-$) are negligible, while at pH 1, anionic species represents less than 13% (decreasing almost linearly with pH until reaching stable fraction close to 0.75% at pH 3 and above). At pH 1.5–2, NdSO_4^+ represents about 76% of total species ($\approx 19\%$ for Nd^{3+}), while above pH the distribution between cationic sulfate species and free Nd^{3+} species stabilizes around 56.6% and 42.5%, respectively.

The pH-edge profiles of Nd(III) sorption are similar for Mono-AP and Bis-AP (Fig. 4): the sigmoid curves begin with negligible sorption capacities (less than 0.07 mmol/g) at $\text{pH}_{\text{eq}} 1.21\text{--}1.50$ (Nd(III) probably bound under anionic form). In acidic solutions, the Bis-AP shows little higher efficiency in neodymium removal (probably because there is a higher density of active functional groups). Sorption slightly increases with increasing the pH, (as a result of the competing effects between protons) neodymium being sorbed as anionic species (below pH 3) and by proton exchange (with free Nd^{3+} and NdSO_4^+) and by complexation with phosphonate moieties. The sorption capacity progressively and sharply rises above $\text{pH}_{\text{eq}} 3$ and up to $\text{pH}_{\text{eq}} 5$.

This may be a result of the progressive decrease of reactive group's protonation, the decreased competition of protons (especially above pH 4). Regarding the two sorbents the differences in sorption capacities between the two sorbents are negligible. At $\text{pH}_{\text{eq}} 5$, the sorption capacity stabilizes for Mono-AP, while it continues increasing up to $\text{pH}_{\text{eq}} 5.8$ for Bis-AP (where q_{eq} stabilizes). The stabilization in sorption capacity for different pH values can be related to the sorbents' acid-base characteristics (surface charge): the pH stabilization change corresponds to the shift in pH_{PZC} values. Several studies have demonstrated the significance of the phosphonate group environment for the sorption properties of

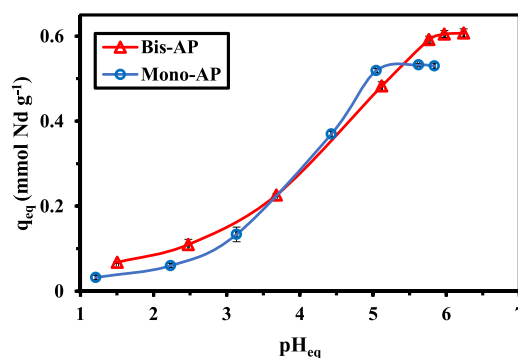


Fig. 4. Effect of pH on Nd(III) sorption using Mono-AP and Bis-AP (C_0 : $0.35 \text{ mmol Nd L}^{-1}$; SD: 0.5 g L^{-1} ; T: 25°C ; Time: 2 h; v : 200 rpm).

relevant sorbents [51–53]: these investigations stressed the donating effect of auxiliary groups on the sorbents' affinity to target ions. In the case of the complexation of divalent cations by phosphonomethylcholine, the effect of charge hold by distant methylammonium groups was highlighted [71]: the stability constants are linearly correlated with the ligand acid-base characteristics (i.e., pK_c vs pK_a). In the case of phosphate-bearing sorbents, Alexandratos and Zhu [72] correlates the binding capability of PO moieties to metal ions with the abundance of lone-pair electrons and the activation effect of hydrogen bonding; this balance is controlled by the proper properties of the auxiliary amine groups vicinal to phosphate groups. They also pointed out the importance of the polarizability of phosphoryl oxygen for the interaction with metal ions (and the greater affinity for trivalent cations opposed to divalent cations in acidic solutions).

In the case of microporous di(2-ethylhexyl) phosphonate impregnated silica-polymer (HDEHP), Sc(III) sorption was reported to increase with sulfuric acid concentration [73], while for other REEs, a maximum sorption was reported with H_2SO_4 concentration from 0.5 to 1 M H_2SO_4 . Zhang et al. correlated this specific behavior to the difference in solvation effect of Sc(III) against other REEs that require higher acidity for expressing this solvation mechanism. For Nd(III) liquid-liquid extraction employing a combination of phosphonic acid/ phosphoric acid ester extractant (HDEHP/HEH-EHP), the extraction efficiency continuously increased with pH (below precipitation region) [74]. Similar trends were reported for Pr(III) extraction using a mixture of ionic liquid (A336/ NO_3 and a phosphonate based extractant (DEHEHP) [75]. Burdzy et al. presented a comprehensive comparison of REEs sorption in presence of citrate anions by a series of ion-exchange and chelating resins [76]. Based on the speciation of Nd(III) ions, substantial changes were reported. Hence, for chelating ion exchangers (such as Purolite S957) the adsorption performance was hardly affected by the solution pH. For Purolite S950 (chelating resin), and Lewatit SP112 (cation exchanger), the formation of Nd-citrate complexes (with pH increase) decreases sorption affinity, while for Amberlite IRA 67 (anion exchanger) a maximum sorption was observed at pH 4. For strongly basic anionic exchangers (Lewatit M500, M600, MP500, Amberjet 4200, 4400, 4600, and amberlite IRA 458 and IRA 958), the sorption is depreciated in acidic solutions because of charge repulsion between predominant cationic species and positively charged binding sites on the resins. These results led to large variations in the selection of the sorption pH that is optimum for individual metals for the different resins; this also opens the route for metal separation (in relation with metal speciation as well as intrinsic characteristics of the resins and).

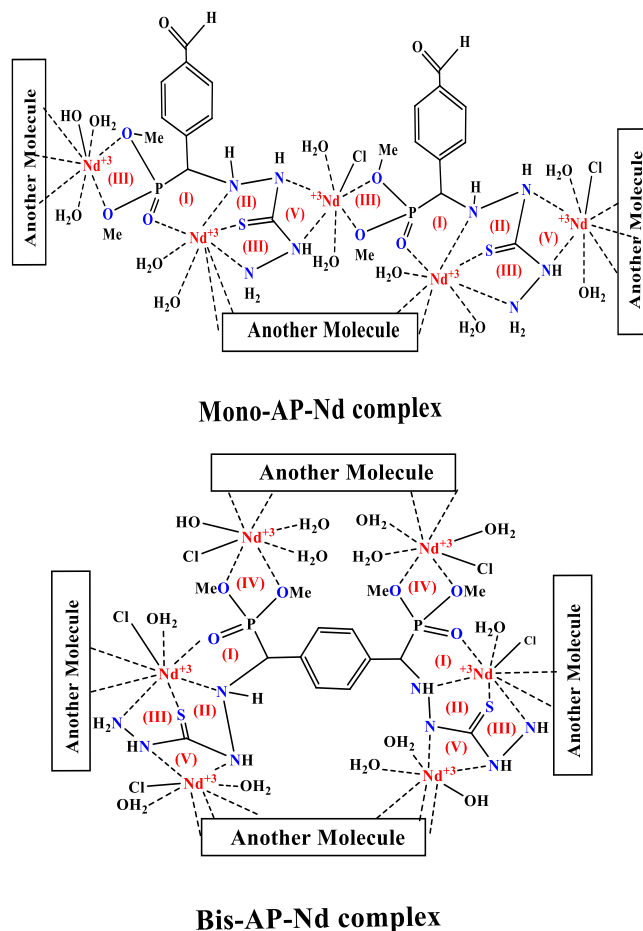
Fig. S2 compares the evolution of equilibrium pH for Mono-AP and Bis-AP; generally, the pH increases after metal sorption (the weakest variations are obtained at pH_0 : 6.05). The largest pH increase is obtained at pH_0 4.54–5.04 (consistently with the titration of the sorbent in the determination of the pH_{pZC} , not shown). The pH increase is significantly highly noticed for Bis-AP (+1.22) than for Mono-AP (+0.59) (Consistently with the sorbents acid-base characteristics). The pH_{eq} is consistently increased with neodymium sorption onto the sorbents that is highly recognized for Bis-AP (as a result of the greater amount of functional groups which in turn may bind extra Nd(III) ions). The diversity of the pH can be attributed to the dissolution of –OH moieties (at high pH levels) due to potential mechanism of ligand interchange around the level of neodymium species and/or the simultaneous proton binding with neodymium. The same trends were observed for uranyl sorption onto similar aminophosphonate-based sorbents [51].

In the La(III) solvent extraction by two phosphonate-based extractants, the equilibrium pH decreased after extraction because of the ion exchange mechanisms (between La^{3+} and protons): involving the decrease of the pH. The sorption of neodymium may involve ion-exchange mechanisms (on proton-exchangeable sites and/or protonated functional moieties) and chelation (which may also be accompanied by proton exchange). The pH_{eq} plot vs. log of distribution ratio (D , $L \cdot g^{-1}$, q_{eq}/C_{eq}) is reported in Fig. S3. This graph is typically employed to

identify the proton interchange ratio within ion-exchange processes (slope of $\log_{10} D$ vs. pH_{eq}); by extension this is employed here to correlate the sorption with the displacement of protons. The slope is varying between + 0.39 for Bis-AP and + 0.44 for Mono-AP. This slope ($\approx +0.4$) is dis-correlated with the potential stoichiometric ratio between reactive groups and metal species; the result indicated that the sorption process is not simple one that proceeds through different modes on interactions involving active functional moieties and/or different species. In the situation of REEs extraction with R_4N^+ -EHEHP, Quinn et al. also reported that the slope values (i.e., +1.5/+2.2) were systematically lower than the expected value (i.e., +3) [77]. On the opposite hand, Huang et al. compared different phosphonate-based extractants for La(III) recovery from aqueous solutions; the slope analysis showed a consistent + 3 slope that confirmed the simple ion-exchange process [78].

Based on the characterization of the interactions of the sorbents with Nd(III) through pH effect and the XPS and FTIR analysis, the potential tentative mechanisms for Nd(III) binding onto the sorbents are shown in Scheme 1. Virtanen et al. proposed different zwitterionic structures for the complexation of REEs with bis-aminophosphonate ligand (depending on the metal/ligand stoichiometric ratio, which is conditioned also by the solution pH) [79]. The coordinating sphere may involve 2 H_2O molecules (at 1:1 ratio), 2 amino moieties and two phosphonate groups, while at higher M/L ratio, the contributions of H_2O and amino progressively decreased (i.e., 1 molecule), at M/L 1:2, and disappeared at M/L 1:3, being progressively replaced with phosphonate (i.e., RP-O⁻ moieties).

As well, the bonds established between Ln^{3+} ions and ligands are of electrostatic nature, and stable complexes are exclusively achieved with



Scheme 1. Tentative mechanisms for the binding of Nd(III) on Mono-AP and Bis-AP sorbents.

polydentate chelating ligands. Similar to the aquo ions $[\text{Ln}(\text{OH}_2)_n]^{3+}$, the coordination numbers of complexes vary throughout the series. For instance, the smaller Yb^{3+} forms a 7-coordination complex $[\text{Yb}(\text{aca-c})_3(\text{OH}_2)]$, whereas the larger La^{3+} forms an 8-coordination complex $[\text{La}(\text{aca-c})_3(\text{OH}_2)_2]$ [80]. Moreover, Dudarko et al. [42], reported that Nd(III) ions can coordinate with various interaction modes, encompassing coordination numbers 8 and 9. Thus, Nd(III) forms 8-coordination complexes within a single ligand molecule and/or between two molecules (Scheme 1).

3.2.2. Uptake kinetics

Fig. 5 represents kinetic curves. Time ($t_{\text{equilibrium}}$) hardly changes with the type of sorbent. During 60–90 min, the equilibrium is attained. This means that the textural characteristics of the sorbents (size, pore size, porosity, and surface area) have limited effect on mass transfer properties. As expected, the increased active groups amount improved neodymium sorption: the residual relative concentration slightly decreases (from 0.33 to 0.26 for Mono-AP to Bis-AP, respectively). For the Ln(III) adsorption (i.e., Nd(III), Ce(III) and La(III)) onto composite biochar, Kolodynska et al. reported equilibrium times close to 120 min [81]. Park and Tavlarides synthesized a phosphorus based sol-gel sorbent and reported equilibrium times close to 120–150 min for Nd(III) sorption [36].

Sorption kinetics may be affected by the physical properties of the sorbent (in terms of diffusion procedures, such as resistance to intraparticle, film and bulk diffusion), the process parameters (agitation speed, temperature) but also the proper reaction rate of the sorption at molecular level (herein considered through PFORE and PSORE t , i.e., the pseudo-first and pseud film and bulk resistances diffusion may be ignored (except at short contact time), more attention is thus paid towards intraparticle diffusion mechanism (RIDE, Crank equation, [82]). A reminder of conventional equations is shown in Table S1. The statistical criteria and the fitting parameters (with the three models) of empirical curves for the two sorbents are compared in Table 1. For Mono-AP sorbent, the PFORE fits better kinetic curves (as indicated by both the AIC (Akaike information criterion), and R^2 (the determination coefficient)). For Bis-AP, the three models cannot be distinguished as the differences between the AIC values $|\Delta(\text{AIC})|$ are insufficiently large (the should exceed 2). However, the PFORE allows closer evaluation (underestimated by less than 1.5%, while for the PSORE model q_{eq} is overestimated by 10.4–8.9%) as shown by the contrast between experimental q_{eq} values and calculated ones. Fig. 5 shows PFORE experimental profiles represented by solid lines while Fig. S4 reports the RIDE and the RIDE fits. As expected from the trends observed in Fig. 5, the bis-phosphonation weakly increases the k_1 (apparent rate coefficient): the k_1 value increases from 6.6×10^{-2} to $8.0 \times 10^{-2} \text{ min}^{-1}$. The value of k_2 ranges between 0.15 and $0.17 \text{ g mmol}^{-1} \text{ min}^{-1}$; this is smaller than the value ($1.59 \text{ g mmol}^{-1} \text{ min}^{-1}$) reported for Nd(III) sorption onto composite biochar [81] or ($2.62 \text{ g mmol}^{-1} \text{ min}^{-1}$) for

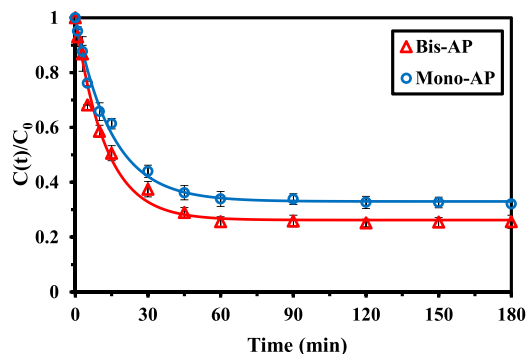


Fig. 5. Uptake kinetics for Nd(III) recovery using Mono-AP and Bis-AP – Modeling with the PFORE (C_0 : $0.35 \text{ mmol Nd L}^{-1}$; SD: 0.5 g L^{-1} ; pH_0 : 4.5; T: $25 \text{ }^\circ\text{C}$; v : 200 rpm).

Table 1

Uptake kinetics for Nd(III) sorption using Mono-AP and Bis-AP – Model parameters.

Model	Parameter	Unit	Mono-AP	Bis-AP	
Experimental	$q_{\text{eq,exp}}$	mmol g^{-1}	0.518	0.571	
	PFORE	$q_{\text{eq,1}}$	mmol g^{-1}	0.511	0.563
		k_1	min^{-1}	0.066	0.080
		R^2		0.995	0.991
PSORE	AIC		-98	-89	
	$q_{\text{eq,2}}$	mmol g^{-1}	0.572	0.622	
	k_2	$\text{g mmol}^{-1} \text{ min}^{-1}$	0.150	0.170	
	R^2		0.992	0.990	
RIDE	AIC		-93	-88	
	$D_e \times 10^{14}$	$\text{m}^2 \text{ min}^{-1}$	3.8	1.8	
	R^2		0.993	0.991	
	AIC		-93	-89	

organophosphorous extractant-impregnated silica-polymer composite [83]. For alginate/clinoptilolite composite, the k_2 values significantly decreased with increasing concentration of Nd(III) (from 0.72 to $0.010 \text{ g mmol}^{-1} \text{ min}^{-1}$ with C_0 : $25\text{--}200 \text{ mg Nd L}^{-1}$; i.e., $0.17\text{--}1.39 \text{ mmol Nd L}^{-1}$) [84]. The RIDE allows approaching the sorbent's effective diffusivity value (D_e , $\text{m}^2 \text{ min}^{-1}$, derived from the Crank equation). Despite the relatively fast kinetics, it was expected that shorter equilibrium time can be achieved by reducing the micro-particles size of the sorbent. This indicated the non-negligible effect of the intraparticle diffusion resistance on the resistance control. The magnitude order of D_e (from 1.8×10^{-14} to $3.8 \times 10^{-14} \text{ m}^2 \text{ min}^{-1}$) confirmed this indication. This is significantly less than the Nd(III) free diffusivity ($3.70 \times 10^{-8} \text{ m}^2 \text{ min}^{-1}$) in aqueous solutions [85], as an affirmation of the contribution of intraparticle diffusion resistance in Nd (III) sorption as well as PFORE (proper reaction rate). For alginate/clinoptilolite composite, Fila et al. reported effective pore diffusivity decreasing in the range ($9.1 \times 0.97 \times 10^{-16} \text{ m}^2 \text{ min}^{-1}$) with increasing metal concentration) [84].

3.2.3. Sorption isotherms

The Nd(III) adsorption isotherms by Mono-AP and Bis-AP at different temperatures are shown in Fig. 6. The sorption isotherms (representing q_{eq} vs. C_{eq}) allow reaching other characteristics of the interactions between metal ions and sorbents: (a) the q_m , mmol Nd g^{-1} (maximum sorption capacity), and (b) the sorbent's tendency to bind to a particular metal (correlated to the isotherm curve's initial slope, which is derived from Eq. 6).

$$\left[\frac{\partial q(C_{\text{eq}})}{\partial C_{\text{eq}}} \right]_{C_{\text{eq}}=0} = q_{m,L} \times b_L \quad (6)$$

Where $q_{m,L}$ and b_L are the constants of the Langmuir equation (See Table S1) [86]. The sorption homogeneity is assumed by the Langmuir equation (involving interactions of the same energy between the metal ions and the sorption sites), without multilayer coverage and without interactions between sorbed molecules. The equalization of desorption and sorption ratios manifested the mechanistic of Langmuir equation. A quasi linear initial slope following by a curved section and a final asymptotic trend (which corresponds to the saturation plateau) are the systematic characteristics of sorption isotherms. The existence of this plateau dismisses Freundlich equation employment to fit the experimental profile (Table S1), empiric equation associated with heterogeneities in the adsorption energies and lateral interactions among adsorbed molecules. Freundlich equation was tested but AIC as well as R^2 values confirmed that this equation fails to fit experimental curves (not shown). The Freundlich and equations are combined in the Sips equation (see Table S1) that generally allows reaching a better fit of the curves section of the isotherm. The mathematical fitting of the empirical profile is simplified by the introduction of the third-adjustable parameters (though the physicochemical significance of the model is lost). The

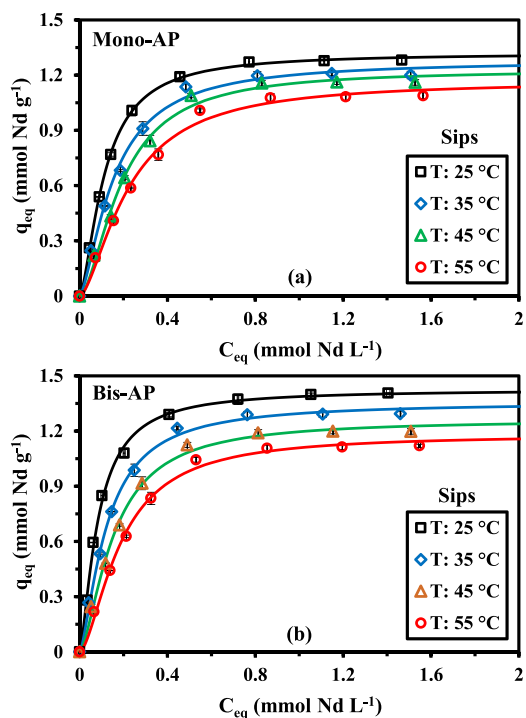


Fig. 6. Nd(III) sorption isotherms using Mono-AP (a) and Bis-AP (b) at different temperatures – Modeling with the Sips equation (C_0 : 0.18–2.12 mmol Nd L⁻¹; SD: 0.5 g L⁻¹; pH₀: 4.5; T: 25 °C; Time: 1 h; v- 200 rpm).

Sips fitting represented by solid lines is reported in Fig. 6 whereas the Langmuir fits appear in Fig. S5 (for comparison). Table 2 compares the statistical criteria as well as the parameters for the two sorbents applying Langmuir as well as Sips equations at different temperatures. Compared with Langmuir equation, the experimental data are highly correlated with the Sips equation.

The isotherm calculations were executed to obtain the predicted removal efficiencies as a function of the mass of both Mono-AP and Bis-AP sorbents for the different ranges of Nd(III) ions concentrations. This indicates that the required Mono-AP and Bis-AP weights for any range of concentrations could be pre-estimated prior to the actual sorption process. Namely, the weight of Mono-AP and Bis-AP required to intake Nd(III) ions in a concentration range (from 0.18 to 1.43 mmol L⁻¹) in one-liter volume solution was calculated to be 0.517 and 0.509 g L⁻¹, respectively at 25 ± 1 °C (according to the Sips parameters equation nonlinear form, in Table 2). These mass values align with the sorption capacities of these sorbents.

The Temkin equation (Table S1) was also unsuccessful (not shown); this model supposes the binding to proceed through multilayer with

interactions between the sorbent and the sorbate (with the linear decrease of the sorption heat via surface covering) [87]. D-R (the Dubinin-Radushkevich equation), originally designed to simulate sorption isotherms in solid/gas systems was extended to solid/liquid equilibria. Usually, this equation is employed for discussing the mode of interaction discriminating between physisorption and chemisorption. Recently, Puccia et al. comprehensively discussed the literature and showed that for solid/liquid systems, the discrimination based on the absolute value of the energy of adsorption is critically oriented by the units of concentrations used for modeling: molar unit systematically drives to chemical adsorption conclusion while mg L⁻¹ unit leads to physical sorption [88]. Therefore, they suggest restricting the ambition of the calculation to mathematical fit and comparative analysis. Herein, Table S8 and Fig. S6 display the sorption isotherms fits by D-R equation; though the fits were worse than for Langmuir and Sips equations, the D-R equation is more appropriate than Freundlich and Temkin models.

Table 2 (and Table S8) and Fig. 6 both confirm that the bis-functionalization slightly increases sorption properties compared with mono-functionalization: $q_{m,exp}$ (the maximum adsorption capacity) increases by 9.6% at T: 25 °C. It is noteworthy that this benefit progressively decreases with increasing temperature; at T: 50 °C, the enhancement is less than 3%. Similar trend is observed for $q_{m,S}$ (decrease from 8.1% to 1.0%). This is a first indication that the thermodynamics of Nd(III) sorption on Mono-AP and Bis-AP are not following the same trends. Comparing b_L and b_S (affinity coefficients) reveals substantial increase with the bis-functionalization; however, the improvement is not “homogeneous” (between 11% and 39%); it depends on the model used and the temperature. The sorption exothermicity is indicated by the sorption capacity reduction by rising temperature; the enthalpy change calculation affirmed this indication (ΔH° , kJ mol⁻¹, derived by the van’t Hoff (Eq. 7) application) [89]:

$$\Delta G^\circ = -RT \ln K_{eq}^0 = \Delta H^\circ - T\Delta S^\circ \quad (7a)$$

$$\ln K_{eq}^0 = -\frac{\Delta H^\circ}{R} \times \frac{1}{T} + \frac{\Delta S^\circ}{R} \quad (7b)$$

$$\text{With : } K_{eq}^0 = b_L^* \times \frac{C_{Sorbate}^0}{\gamma_{Sorbate}} \quad (7c)$$

And ΔS° , entropy change in J mol⁻¹ K⁻¹; ΔG° , free Gibbs energy change in kJ mol⁻¹; R: gas constant; $C_{Sorbate}^0$, unitary standard concentration of sorbate (≈ 1 mol L⁻¹), b_L^* , the Langmuir constant in L mol⁻¹ unit; and $\gamma_{Sorbate}$: dimensionless activity coefficient (≈ 1 for diluted solutions).

Based on Table 2 and Fig. S7, it was possible determining the different thermodynamic variables which are listed within Table 3. The exothermic nature of Nd(III) sorption on Mono-AP and Bis-AP is confirmed by enthalpy change negative values (–21.8 and –24.6 kJ mol⁻¹, respectively). The two sorbents have comparable

Table 2
Effect of temperature on Nd(III) sorption isotherms for Mono-AP and Bis-AP – parameters for Langmuir and Sips equations.

Sorbent	Parameter	T (°C)	Mono-AP				Bis-AP			
			25	35	45	55	25	35	45	55
	$q_{m,exp}$ (mmol Nd g ⁻¹)		1.282	1.210	1.163	1.088	1.405	1.294	1.198	1.120
Model			Langmuir							
	$q_{m,L}$ (mmol Nd g ⁻¹)		1.470	1.440	1.453	1.386	1.550	1.496	1.430	1.378
	b_L (L mmol ⁻¹)		7.269	5.205	3.889	3.294	10.16	6.883	5.232	4.074
	R ²		0.986	0.984	0.977	0.980	0.990	0.988	0.984	0.981
	AIC		-46	-46	-43	-60	-47	-48	-46	-60
Model			Sips							
	$q_{m,S}$ (mmol Nd g ⁻¹)		1.319	1.280	1.223	1.170	1.426	1.356	1.263	1.182
	b_S (L mmol ⁻¹) ^{ns}		29.70	15.80	16.26	10.98	36.19	21.21	18.10	15.22
	ns (-)		0.642	0.674	0.593	0.629	0.694	0.690	0.647	0.617
	R ²		1.000	0.995	0.994	0.994	0.998	0.998	0.996	0.997
	AIC		-74	-52	-51	-69	-58	-59	-55	-75

Table 3

Thermodynamic parameters for Nd(III) sorption on Mono-AP and Bis-AP sorbents.

Sorbent	Mono-AP			Bis-AP		
	ΔH^0	ΔS^0	ΔG^0	ΔH^0	ΔS^0	ΔG^0
Temperature (°C)						
25	-21.76	-0.71	-21.55	-24.60	6.0	-26.40
35			-21.54			-26.46
45			-21.53			-26.52
55			-21.53			-26.58

Units: ΔH^0 and ΔH^0 , kJ mol⁻¹; ΔH^0 , J mol⁻¹ K⁻¹.

enthalpy changes. It is noteworthy that the entropy change is negligible for Mono-AP (i.e., -0.7 J mol⁻¹ K⁻¹) and very low for Bis-AP (about 6 J mol⁻¹ K⁻¹). Consequently, ΔG^0 is poorly affected by temperature, varying from the mono-sorbent (-21.5 kJ mol⁻¹) to the bis-sorbent (-26.5 kJ mol⁻¹). The sorption spontaneity and feasibility are indicated by the ΔG^0 negative values. Low values of ΔS^0 indicate that the sorption randomness is poorly affected by the sorption mechanism: almost unchanged for Mono-AP and little increase in randomness for Bis-AP. These changes in thermodynamic trends can be explained by different mobility in water exchange and ion-exchange, as involved in Nd(III) sorption (on either the sorbent or the metal species).

Table 4 compares Nd(III) sorption properties of Mono-AP and Bis-AP with a series of alternative sorbents. The optimal pH value, the required contact time for equilibrium, and Langmuir parameters (in addition to experimental maximum sorption capacity) are reported. Obviously, the global performance is influenced by the pH, the temperature (herein, the values are systematically for temperature in the range 20–25 °C), the sorbent dose (for kinetics). Despite this variability, Table 4 helps in getting a rapid overview on the relative potential of these sorbents. Two materials show outstanding performances for neodymium removal from aqueous solutions: (a) with graphene oxide/carboxymethyl cellulose, $q_{m,exp.}$ is up to 4.58 mmol Nd g⁻¹ at pH 3 [90] (with low affinity coefficient), and (b) around 3.54 mmol Nd g⁻¹ at pH 5 with magnetic glutamine-derivative of polyacrylonitrile/divinyl benzene sorbent [91]. Though the textural properties of the graphene oxide derivative have not been characterized [90], it is well known that exfoliated graphene oxide materials exhibit outstanding specific surface area (typically higher than 2000 m² g⁻¹, which is probably significantly reduced after grafting CMC); this may contribute to the high levels of sorption together with the high density of carboxylate groups. For the magnetic glutamine

Table 4

Comparison of Nd(III) sorption properties with alternative sorbents.

Sorbent	pH	Time	$K_1/OR K_2^*$	$q_{m,exp.}$	$q_{m,L}$	b_L	Ref.
<i>Kluyveromyces marxianus</i>	1.5	1440	-	0.063	0.083	5.62	[108]
Magnetic phosphonic extractant-loaded alginate beads	4	600	6.49	-	1.035	4.90	[96]
Aminomethylphosphonic derivative of chitosan	5	420	5.05	0.201	0.409	7.79	[109]
<i>Chlorella vulgaris</i> algae	5	90	1.01	-	1.308	4.18	[110]
Ionic liquid impregnated silica	3.5	180	0.022 min ⁻¹	0.095	0.102	23	[98]
Magnetic glutamine-derivative PAN/DVB	5	60	3.06 min ⁻¹	3.54	3.63	208	[91]
Chitosan/Fe(OH) ₃ composite	4	420	5.63	0.080	0.095	4.33	[93]
Zirconium titanate/PAN	4.5	1440	-	-	0.035	0.98	[111]
Diglycolic acid functionalized polyethylene terephthalate nanofibers	6	100	-	0.876	0.859	0.039	[112]
EDTA/phosphonic bifunctionalized SiO ₂	3.5	60	-	1.56	1.56	7.21	[42]
Phosphoryl-functionalized algal-PEI beads	5	40	1.13	1.46	1.92	1.25	[92]
Purolite A-400 (Cl-form)	6	n.d.	-	0.30	0.69	0.875	[113]
MMA-grafted poly-D-galacturonic acid methyl ester	6	90	0.04 min ⁻¹	-	0.036	47.6	[114]
Straw derived biochar	5	120	-	0.497	0.954	3.74	[115]
Graphene oxide/carboxymethyl cellulose	3	5	-	4.58	4.53	0.0027	[90]
Amino-alkylphosphonic functionalized PGMA	4.5	240	0.411	0.736	0.776	9.59	[99]
Biochar/alginate beads	5	1440	9.81	0.763	0.753	42.0	[84]
Glutenin extract-clay	5.5	60	0.36×10^{-5}	0.361	0.517	11.5	[116]
Amino-based grafted-SiO ₂	5.8	1080	-	0.83	1.12	0.16	[117]
Bentonite	4	30	-	0.25	0.246	83.4	[118]
Mono-AP	4.5	90	0.066	1.28	1.47	7.27	This work
Bis-AP	4.5	90	0.150	1.41	1.55	10.2	This work

n.d.; not documented; Units: time, min; qm: mmol Nd g⁻¹, bL: L mmol⁻¹. *Unit: K1 (in min⁻¹)/OR K2 (in g mmol⁻¹ min⁻¹).

derivative [91], which implies numerous synthesis steps, the density and configuration of grafted amine groups (associated with sulfur-based moiety) may explain the high levels of sorption. Apart these two sorbents and in a spectrum of 1.2 – 1.6 mmol Nd g⁻¹, a group of materials show comparable sorption capacities. In addition to Mono-AP and Bis-AP, phosphorylated algal-PEI beads shows good sorption capacity ($q_{m,exp.}$: 1.46 mmol Nd g⁻¹), with medium affinity (b_L : 1.25 L mmol⁻¹), and fast kinetics (equilibrium time: 40 min) [92]. Dudarko et al. showed the remarkable improvement of sorption performance with the post-functionalization of EDTA-grafted SiO₂ sorbent [42]: the conformation of the sorbent (arrangement of different functional moieties: carboxylate, phosphonate and amine groups) at pH 3.5, allowed increasing the $q_{m,exp.}$ value from 0.329 to 1.56 mmol Nd g⁻¹ (while the affinity coefficient remains unchanged). Bis-AP and Mono-AP exhibit promising global sorption properties.

3.2.4. Metal desorption and sorbent recycling

An important criterion especially in designing complex adsorbents is the metals desorption for adsorbent recycling. In many cases the neodymium sorption is favored by mild acidic or neutral pH values; therefore, shifting the pH to stronger acidic conditions may be used for reversing the sorption process and eluting target metal. Hence, HCl solutions were frequently used for chitosan/iron(III) hydroxide for the elution of Nd(III) at pH 3.5 [93], pH 1–1.8 solutions in the case of alginic acid beads [94], pH 1 solutions for *Sargassum* sp. biomass [95] or extractant-impregnated magnetic alginate microcapsules [96]. In the case of alginate-silica composite, to achieve the complete Nd(III) desorption, HCl concentration was raised to 0.5 M [97]. For neodymium desorption, Mohamed et al. utilized a 1 M HNO₃ solutions to completely elute Nd(III) from ionic liquid-impregnated silica material [98]. Nitric acid concentration was decreased to 0.5 M for metal desorption in the case of phosphonate-functionalized PGMA [99]. Lower nitric acid conditions (i.e., 0.1 M) were sufficient for Nd(III) elution from Loquat leaves [100]. In the case of expanded vermiculite, Brião et al. used 0.3 M CaCl₂ solutions (based on Nd(III)/Ca(II) ion-exchange) [101,102]: calcium-based desorption was little more efficient than 0.1 M nitric acid solution. For the desorption of U(VI) from chitosan derivatives bearing α -aminophosphonate (AP) moieties, 0.05 M sodium bicarbonate solutions were successfully used; in this case the affinity of uranyl for forming stable complexes was privileged.

Herein, the sorption involving ion-exchange and chelation

mechanisms suggests using acidic solutions for Nd(III) elution. Hydrochloric acid solution of moderate concentration (i.e., 0.2 M) was selected for evaluating the possibility to reuse the sorbent for six successive cycles. Table 5 demonstrates that throughout the materials recycling, sorption and desorption efficacies gradually and lightly decline. The variability in performances is comparable for the two sorbents: at the sixth cycle, the sorption loss represents 7.5% and 6.4% for Mono-AP and Bis-AP, respectively. The stability of the sorbent is little better when the material is bis-functionalized. The differences are insignificant in terms of desorption. These results are confirmed by the weak evolution of the FTIR (see Section 3.1.2.) while the sorbent is reused. In the case of alginate-silica sorbent, the sorbent loss about 20% of its sorption efficiency at the first recycling, while the sorption levels are weakly affected for the next six cycles [97]: this was explained by a change in the conformation of the biopolymer under acidic conditions (alteration of the structure driven by the egg-box model with Ca(II) in sorbent synthesis). For extractant-impregnated magnetic alginate beads, Zhang et al. reported a continuous loss in sorption and desorption efficiencies at recycling [96]; the loss reaches at the third cycle $\approx 10\%$ and $\approx 5\%$, respectively. This was explained by the incomplete desorption that contributes to decrease the amount of available functional moieties. For expanded vermiculite, the sorption efficiency was remarkably stable for five cycles; despite large variations in the desorption yield (especially during the first cycles; variability explained by the release of other remaining ions) [102]. The Mono-AP and Bis-AP interest in for recovering REEs such as neodymium from aqueous solutions is confirmed by the good stability of these sorbents with regard to sorption and desorption efficiencies. Based on the experimental conditions (respective volumes of sorption phase and eluent phase), the concentration effect is limited to 2:1; for practical applications this would require investigating more deeply the $V_{\text{sorption}}/V_{\text{desorption}}$ criterion.

3.3. Nd(III) dynamic studies

The essential factor for the practicality of a potential sorbent in sorption processes lies in its capacity to function effectively within a continuous system (i.e., columns method). However, the particle size is not compatible for practical application in fixed-bed columns, due to particle size so thin that filled column would be associated with blockage, head loss pressure. Based on the current conditioning of the sorbent (as microparticles) the study in fixed-bed reactor would only be possible in shallow bed reactor (which are poorly representative of practical application) [103], or with fluidized bed reactor [104]. For practical application two possibilities are opened: (a) combining the polymer with magnetic core (for facilitating practical solid/liquid separation after sorption step) for application in batch reactor, or (b) agglomerating (granulating)/encapsulating the microparticles (at the expense of probable kinetic limitations due to resistance to diffusion) for fixed-bed application. This work is thus more oriented toward the interpretation of the effect of synthesis conditions (molar ratio of precursors) and optimization of sorption properties (in relation with the structure of the sorbents). The evaluation of synthesis conditions and the demonstration of the merits of optimized sorbent open the way to

further developments of conditioned sorbents with practical target.

Herein, a simple and rapid column experiment (This test is merely a preliminary investigation and will be considered in future work) was conducted to assess the practical applications in treating aqueous effluents. For the preparation of a free-standing column involves the use of a one-milliliter (1 mL) syringe. 0.25 g of each sorbent powder was well-mixed with 0.5 g of sand (size fraction below 125 μm) to enhance the porosity in a one-milliliter syringe (1 mL, internal diameter (\varnothing): 4.606 mm)) to get sample column for a small test for dynamic adsorption experiments. Notably, glass wool is placed at the bottom of the syringe to prevent sorbent and sand from escaping the column. Under a set of conditions (C_0 : 0.711 mmol L⁻¹, pH₀: 4.0, Temperature: 25 ± 1 °C, and flow rate 40 mL h⁻¹) for 300 mL Nd(III) solution. This experiment resulted in an approximately 99.7% removal efficiency for both sorbents. This rapid test provides meaningful and effective results for real-world applications.

3.4. Metal recovery from ore leachate

3.4.1. Pre-treatment of real industrial solution

Table S9 displays the monazite ore concentrate composition: the total fraction of REE-oxides represents up to 76%. The concentrate acidic leaching produces a pregnant liquor solution (PLS) containing a wide variety of REEs. In terms of mass fraction, cerium is the predominant REE (29.5%), together with neodymium (15.2%) and lanthanum (14.1%). Light REEs (LREEs), which includes also Pr(III) (9.1%), Pm(III) and Sm(III) (6.7%) represent about 75%. Among heavy REEs (HREEs), the most important elements are Y(III) (8.0%), Gd(III) (7.2%), and Dy (III) (6.1%). The PLS was diluted and precipitated at pH 5.8–6 using alkali/ammonia solution. This pre-treatment leads to partial precipitation of Ce(III), which is present at high concentration in the leachate. During this operation, substantial amounts of REEs are lost: from 15–17% for Gd(III) and Y(III), to 53–61% for Ce(III), Yb(III), and Lu(III). Neodymium loss does not exceed 12%. In PPLS, the major elements are Ce(III) (20.5%), Nd(III) (19.2%), and Y(III) (15.5%).

3.4.2. Recovery of Nd(III) from pre-treated leachate

In Table S9, the residual concentrations (after sorption step) are compared for Mono-AP and Bis-AP. The trends are similar for the two sorbents, Bis-AP recovers the REEs with little higher efficiency than the mono-functionalized material. Apparently, the most significant differences between the two sorbents are registered for LREEs; hence, the differential effect of the functionalization is negligible for HREEs. This table also shows that the efficiency of Bis-AP decreases according the series: Nd > La > Pr > Ce > Eu > Yb > Lu > Gd ~ Sm > Dy \approx Y. With the exception of Sm(III), the sorbents fixed better LREEs than HREEs, under selected experimental conditions. The semi-quantitative EDX investigation for the adsorbents collected following the PPLS treatment before and after calcination (Table S10) affirmed these results. This overall observation motivates a deeper study of the selectivity properties. Fig. 7 illustrates different representations through the comparison of sorption capacities, distribution ratio and $SC_{\text{metal}/\text{Nd}}$, which is defined as:

Table 5

Performances of sorption and desorption for 6 successive cycles of re-use.

Sorbent Operation Cycle	Mono-AP			Bis-AP				
	SE (%) Aver.	St. Dev.	DE (%) Aver.	St. Dev.	SE (%) Aver.	St. Dev.	DE (%) Aver.	St. Dev.
1	100.00	0.00	97.88	0.31	100.00	0.00	98.48	0.18
2	96.92	0.13	97.70	0.10	97.94	0.56	97.67	0.40
3	95.82	0.49	96.99	0.21	96.89	0.41	96.95	0.19
4	94.87	0.80	96.56	0.50	95.53	0.08	96.18	0.14
5	93.06	1.20	95.25	0.54	94.57	0.02	95.20	0.11
6	92.51	0.34	93.55	0.16	93.58	0.14	94.08	0.03
6th vs. 1st	-7.49		-4.33		-6.42		-4.401	

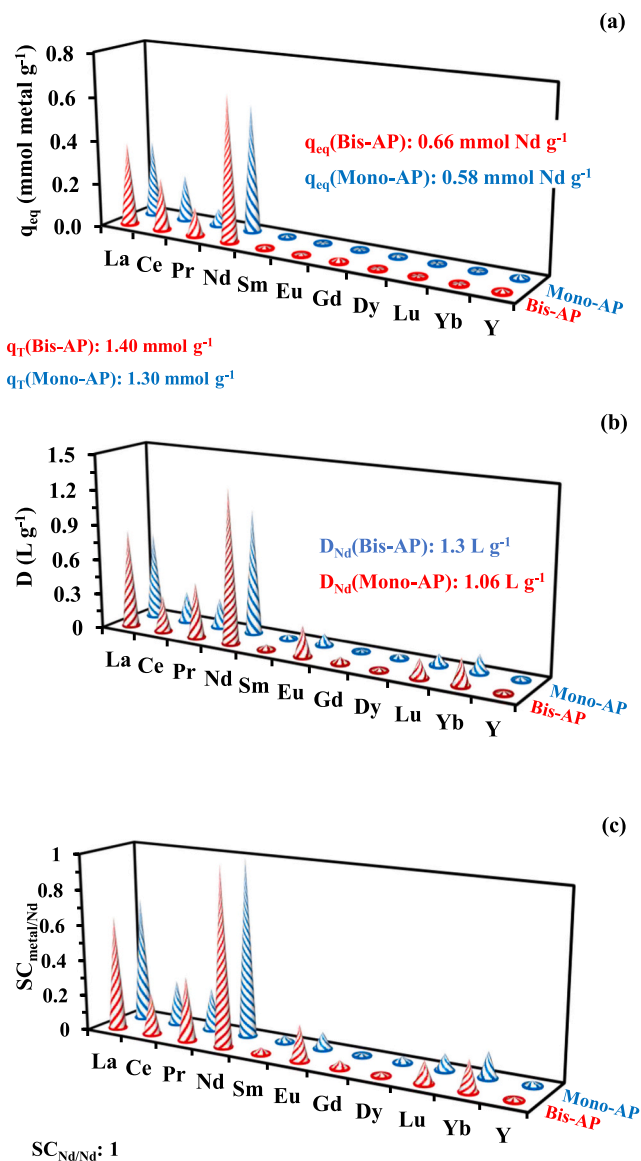


Fig. 7. Recovery of REEs from pre-treated ore leachate using Mono-AP and Bis-AP – Comparison of sorption capacities (a), distribution ratio (b), and selectivity coefficients $SC_{\text{Metal}/\text{Nd}}$ ($SC_{\text{Nd}/\text{Nd}}$ as reference) (c) (SD: 0.5 g L^{-1} ; v : 200 rpm; Time: 1 h).

$$SC_{\text{Metal}/\text{Nd}} = \frac{D_{\text{Metal}}}{D_{\text{Nd}}} = \frac{q_{eq,\text{Metal}} \times C_{eq,\text{Nd}}}{C_{eq,\text{Metal}} \times q_{eq,\text{Nd}}} \quad (8)$$

$SC_{\text{Nd}/\text{Nd}} = 1$ is taken as reference; the lower the coefficient, the stronger the Nd(III) sorbent selectivity rather than co-ions.

q_{eq} up to $0.66 \text{ mmol Nd g}^{-1}$ for Bis-AP (little higher than for Mono-AP; ($0.58 \text{ mmol Nd g}^{-1}$)) (Fig. 7a). The accumulative sorption capacity of Bis-AP and Mono-AP rises to 1.40 and $1.30 \text{ mmol Nd g}^{-1}$, respectively; the sorbents are not specific to neodymium. However, the sorbents have marked preference for LREEs: the cumulative sorption capacity of the REEs the most efficiently sorbed (i.e., Nd, La, Ce, and Pr) represent 95–96% of total sorption. The distribution ratio reflects the concentration effect of the sorbents for target metals (Fig. 7b): D values are systematically larger for Bis-AP than for Mono-AP. The highest distribution ratio is systematically found for Nd(III) (for Bis-AP and Mono-AP at 1.3 and 1.06 L g^{-1} , respectively), following the order (among LREEs): $\text{Nd} > \text{La} > \text{Pr} > \text{Ce}$ (to be opposed to the concentration scale in the PPLS: $\text{Ce} \approx \text{Nd} > \text{La} > \text{Pr}$): there is a complete inversion regarding the concentrating effect of Ce. The comparison of the $SC_{\text{Metal}/\text{Nd}}$ values

confirm these trends and also that Bis-AP is relatively less selective for Nd(II) (and others LREEs) than Mono-AP (Fig. 7c). The higher density of reactive groups opens more active sites for the binding of other metals ions; in addition, HREEs are characterized by smaller ionic sizes (references), which allows these REEs to better accommodate the geometry of reactive groups in the modified sorbent.

How correlating the differences in sorption performances with the physicochemical specific properties of REEs? Fig. S8 shows the dispersion of the distribution ratio of REEs (bubble size proportional to D) in the plot frame R_p vs. χ (solution-phase electronegativity, [105]) for the two sorbents. Though the distribution ratios cannot be linearly correlated to these parameters, the sorbents show marked preference for the metal ions having both low χ values (i.e., < 3.2), and high R_p values (i.e., > 1.1). In addition, the Bis-AP appears less selective for these preferred LREEs against members of HREEs such as Eu, Lu and Yb (as shown by larger size of corresponding bubbles). In the case of phosphite skeleton loaded on covalent organic polymers, Ravi et al. reported the preference ranking for selected REEs: $\text{La} < \text{Ce} < \text{Nd} < \text{Eu}$ [106], which was correlated with their decreasing ionic radius (linked to higher coordination). For the precipitation of REEs using alkyl substituted aminobisphosphonates, Virtanen et al. observed a higher efficiency for the precipitation of HREEs compared with LREEs when using alkyl-substituted aminobisphosphonates [79]. They reported that the most favorable separation factor (between adjacent REEs) were obtained for HREEs. These trends are clearly opposed to the conclusions raised for sorption onto Mono-AP and Bis-AP. In Fig. S9, the distribution ratios are plotted against the softness parameters [85], the Shannon ionic radius of hydrated REEs [107], and the enthalpy of hydration [105], for the two sorbents. It is not possible designing a clear (linear) correlation between the recovery of individual metals (D ratio, in PPLS multicomponent solutions) and these specific physicochemical parameters. These panels clearly demonstrate that: (a) distribution ratio cannot be readily correlated with these properties (despite the preference for LREEs), and (b) sorbents show clear preference for neodymium against other REEs.

Two indices have been designed for qualifying the metals according to their covalent and/or ionic behavior [39]:

$$\text{Covalent Index (CI)} : CI = X^2 \times r_H \quad (9a)$$

$$\text{Ionic index (II)} : II = \frac{Z^2}{r_H} \quad (9b)$$

Where r_H the ionic radius of hydrated species, X is the Pauling electronegativity and Z the formal charge of the metal ion (here +3). Fig. S10 confirms that the LREEs are preferentially adsorbed on the sorbents, especially $\text{Nd} > \text{La} > \text{Ce} > \text{Pr}$; these elements are characterized by low values of Ionic Index. The sorption capacity tends to decrease with increasing the II for LREEs with the remarkable exception of neodymium. On the opposite hand, the plot of q vs. CI does not show significant correlation. The CI is not a good “marker” for anticipating the sorption of the REEs on Mono-AP and Bis-AP.

To evaluate the relative benefit of the bis-functionalization, a modulation factor (β) can be calculated as:

$$\beta = 100 \times \left(\frac{D(\text{Bis-AP})}{D(\text{Mono-AP})} - 1 \right) \quad (10)$$

This parameter allows showing that Bis-AP increases the extraction of Nd(III) (compared with Mono-AP) according the series (Fig. S11):

$\text{Gd} > \text{Eu} > \text{Pr} > \text{Lu} > \text{Yb} > \text{Nd} \approx \text{Ce} \approx \text{Sm} \approx \text{La}$, meaning that the sorption of LREEs is less promoted by the increased aminophosphonation (also explaining the lower selectivity). Furthermore, the sorption of yttrium has been decreased, and that of dysprosium event more.

4. Conclusions

The one-pot reaction of trimethylphosphite, *p*-phthalaldehyde and thiocarbazine allowed synthesizing efficient sorbents for uranyl sorption (playing with different molar ratio between reagents). The current work shows the remarkably efficient neodymium recovery from aqueous solutions at moderate pH (around pH 5). The increase in aminophosphonate content (doubling thiocarbazine and trimethylphosphite molar ratio) slightly increases (by $\approx 10\%$) the maximum Nd(III) adsorption capacity. Uptake kinetics is also slightly enhanced, as is the ability of the material to be recycled (during six consecutive cycles of sorption and desorption). Applied to the recovery of REEs from complex solution (a pretreated pregnant liquor solution issued from acid leachate of monazite concentrate), the sorption capacities have been enhanced by the increased amount of active functional moieties. The sorbents show a preferential sorption of light REEs (specifically, for Nd, La, Ce, and Pr, which are naturally more present in the leachate) against heavy REEs. This can be correlated to two major criteria: the ionic radius and the ionic index. It is noteworthy that increasing the density of aminophosphonic groups has an adverse effect on the selectivity (increase in the binding of HREEs). Among LREEs, neodymium shows an outstanding affinity for these sorbents that cannot be correlated with the intrinsic physicochemical properties (i.e., softness, ionic radius of hydrated species, etc.).

Spectral methods (i.e., FTIR and XPS) show a diversity of functional moieties are involved in Nd(III) sorption of Nd(III) (which reflects the structure of the sorbent that bears thiocarbonyl, amino, and phosphonic groups). These reactive groups that belong to different groups in accordance HSAB theory may explain the sorption of Nd(III) through different mechanisms (such as chelation and ion exchange based on the pH (reactive groups deprotonation and speciation effects)). A remarkable stability of the two sorbents has been shown by the sorbents analysis after several adsorption and desorption cycles (reflected by the stability of sorption and desorption efficiencies).

The aminophosphonic adsorbents are highly effective in neodymium removal (even in complex solutions); however, the comparison of Bis-AP and Mono-AP shows that the performance slightly improve by increasing the amount of aminophosphonic moieties but probably not enough to justify the doubling of reagents in the synthesis path.

CRedit authorship contribution statement

Imam Enas A.: Conceptualization, Data curation, Formal analysis, Investigation, Methodology, Software, Validation, Writing – original draft. **Hashem Ahmed I.:** Conceptualization, Resources, Supervision, Validation, Writing – review & editing. **Lu Xingmei:** Conceptualization, Funding acquisition, Investigation, Resources, Supervision. **Tolba Ahmad A.:** Conceptualization, Data curation, Formal analysis, Investigation, Methodology, Supervision, Validation. **Mahfouz Mohammad G.:** Conceptualization, Investigation, Project administration, Resources, Supervision. **Xin Jiayu:** Conceptualization, Formal analysis, Resources, Validation, Writing – original draft. **El-Sayed Ibrahim El-Tantawy:** Conceptualization, Funding acquisition, Investigation, Methodology, Project administration, Resources, Supervision, Validation, Writing – review & editing. **Mohamady Said I.:** Conceptualization, Data curation, Formal analysis, Methodology, Software, Validation. **Ahmed Abdullah A. S.:** Data curation, Formal analysis, Investigation, Methodology, Resources, Visualization. **Galhoum Ahmed A.:** Conceptualization, Data curation, Methodology, Project administration, Resources, Supervision, Validation, Writing – review & editing. **Guibal Eric:** Conceptualization, Data curation, Formal analysis, Investigation, Methodology, Software, Validation, Visualization, Writing – review & editing.

Declaration of Competing Interest

The authors declare that they have no known competing financial

interests or personal relationships that could have appeared to influence the work reported in this paper.

Data availability

No data was used for the research described in the article.

Acknowledgements

This work was financially funded by the National Key R&D Program of China (Nos. 2021YFE0190800), National Natural Science Foundation of China (Nos. 22178343, 22238011), International Partnership Program of Chinese Academy of Sciences (No. 2023VMA0001), and Key R&D projects in Hunan Province (No. 2021SK2047). This paper is based also upon work supported by the Egyptian Science, Technology, and Innovation Funding Authority (STDF) under grant number 43140. Authors also acknowledge Nuclear Materials Authority, Egypt for their support.

Appendix A. Supporting information

Supplementary data associated with this article can be found in the online version at [doi:10.1016/j.colsurfa.2024.133339](https://doi.org/10.1016/j.colsurfa.2024.133339).

References

- [1] D.T. Buechler, N.N. Zyaykina, C.A. Spencer, E. Lawson, N.M. Ploss, I. Hua, Comprehensive elemental analysis of consumer electronic devices: Rare earth, precious, and critical elements, *Waste Manag.* 103 (2020) 67–75.
- [2] H.M. King, REE - Rare Earth Elements and their Uses, *Geology.com*, 2023.
- [3] European Commission, Waste from Electrical and Electronic Equipment (WEEE), in: D.-G.f.E.D. ENV (Ed.), European Commission, Brussels (Belgium), 2023.
- [4] L. Omodara, S. Pitkaaho, E.M. Turpeinen, P. Saavalainen, K. Oravisjarvi, R. L. Keiski, Recycling and substitution of light rare earth elements, cerium, lanthanum, neodymium, and praseodymium from end-of-life applications - a review, *J. Clean. Prod.* 236 (2019) 117573.
- [5] P. Paranjape, M.D. Yadav, Recent advances in the approaches to recover rare earths and precious metals from E-waste: a mini-review, *Can. J. Chem. Eng.* 101 (2023) 1043–1054.
- [6] WHO, Guidelines for Drinking-water Quality (W.H. Organization (Ed.)), WHO, Geneva, Switzerland, 2017.
- [7] W. Leal, R. Kotter, P.G. Ozuyar, I.R. Abubakar, J. Eustachio, N.R. Matandirotya, Understanding rare earth elements as critical raw materials, *Sustainability* 15 (2023) 1919.
- [8] Y. El Ouardi, S. Virolainen, E.S.M. Mouele, M. Laatikainen, E. Repo, K. Laatikainen, The recent progress of ion exchange for the separation of rare earths from secondary resources—a review, *Hydrometallurgy* 218 (2023) 106047.
- [9] R.K. Jyothi, T. Thenepalli, J.W. Ahn, P.K. Parhi, K.W. Chung, J.-Y. Lee, Review of rare earth elements recovery from secondary resources for clean energy technologies: Grand opportunities to create wealth from waste, *J. Clean. Prod.* 267 (2020) 122048.
- [10] A. Royer-Lavallee, C.M. Neculita, L. Coudert, Removal and potential recovery of rare earth elements from mine water, *J. Ind. Eng. Chem.* 89 (2020) 47–57.
- [11] K. Pyrgaki, V. Gemeni, C. Karkalis, N. Koukouzas, P. Koutsovitis, P. Petrounias, Geochemical occurrence of rare earth elements in mining waste and mine water: a review, *Minerals* 11 (2021) 860.
- [12] D. Xia, N.M. Charpentier, A.A. Maurice, A. Brambilla, Q. Yan, J.-C.P. Gabriel, Sustainable route for Nd recycling from waste electronic components featured with unique element-specific sorting enabling simplified hydrometallurgy, *Chem. Eng. J.* 441 (2022) 135886.
- [13] A.A. Maurice, K.N. Dinh, N.M. Charpentier, A. Brambilla, J.-C.P. Gabriel, Dismantling of printed circuit boards enabling electronic components sorting and their subsequent treatment open improved elemental sustainability opportunities, *Sustainability* 13 (2021) 10357.
- [14] D. Talan, Q. Huang, A review of environmental aspect of rare earth element extraction processes and solution purification techniques, *Miner. Eng.* 179 (2022) 107430.
- [15] A. Akcil, Y.A. Ibrahim, P. Meshram, S. Panda, Abhilashb, Hydrometallurgical recycling strategies for recovery of rare earth elements from consumer electronic scraps: a review, *J. Chem. Technol. Biotechnol.* 96 (2021) 1785–1797.
- [16] Z. Chen, Z. Li, J. Chen, P. Kallem, F. Banat, H. Qiu, Recent advances in selective separation technologies of rare earth elements: a review, *J. Environ. Chem. Eng.* 10 (2022) 107104.
- [17] R.D. Abreu, C.A. Morais, Study on separation of heavy rare earth elements by solvent extraction with organophosphorus acids and amine reagents, *Miner. Eng.* 61 (2014) 82–87.

- [18] X. Huang, J. Dong, L. Wang, Z. Feng, Q. Xue, X. Meng, Selective recovery of rare earth elements from ion-adsorption rare earth element ores by stepwise extraction with HEH(EHP) and HDEHP, *Green. Chem.* 19 (2017) 1345–1352.
- [19] N.N. Hidayah, S.Z. Abidin, The evolution of mineral processing in extraction of rare earth elements using liquid-liquid extraction: a review, *Miner. Eng.* 121 (2018) 146–157.
- [20] H. Matsunaga, A.A. Ismail, Y. Wakui, T. Yokoyama, Extraction of rare earth elements with 2-ethylhexyl hydrogen 2-ethylhexyl phosphonate impregnated resins having different morphology and reagent content, *React. Funct. Polym.* 49 (2001) 189–195.
- [21] D. Kim, L. Powell, L.H. Delmau, E.S. Peterson, J. Herchenroeder, R.R. Bhawe, A supported liquid membrane system for the selective recovery of rare earth elements from neodymium-based permanent magnets, *Sep. Sci. Technol.* 51 (2016) 1716–1726.
- [22] A.C. Ni'am, Y.-F. Wang, S.-W. Chen, G.-M. Chang, S.-J. You, Simultaneous recovery of rare earth elements from waste permanent magnets (WPMs) leach liquor by solvent extraction and hollow fiber supported liquid membrane, *Chem. Eng. Process. Process. Intensif* 148 (2020) 107831.
- [23] S. Inan, H. Tel, Ş. Sert, B. Çetinkaya, S. Sengül, B. Özkan, Y. Altaş, Extraction and separation studies of rare earth elements using Cyanex 272 impregnated Amberlite XAD-7 resin, *Hydrometallurgy* 181 (2018) 156–163.
- [24] K.L. Ang, D. Li, A.N. Nikoloski, The effectiveness of ion exchange resins in separating uranium and thorium from rare earth elements in acidic aqueous sulfate media. Part 2. Chelating resins, *Miner. Eng.* 123 (2018) 8–15.
- [25] D. Gomes Rodrigues, S. Monge, S. Pellet-Rostaing, N. Dacheux, D. Bouyer, C. Faur, Sorption properties of carbamoylmethylphosphonated-based polymer combining both sorption and thermosensitive properties: new valuable hydrosoluble materials for rare earth elements sorption, *Chem. Eng. J.* 355 (2019) 871–880.
- [26] S. Virolainen, E. Repo, T. Sainio, Recovering rare earth elements from phosphogypsum using a resin-in-leach process: Selection of resin, leaching agent, and eluent, *Hydrometallurgy* 189 (2019).
- [27] V.N. Rychkov, E.V. Kirillov, S.V. Kirillov, G.M. Bunkov, M.A. Mashkovtsev, M.S. Botalov, V.S. Semenishchev, V.A. Volkovich, Selective ion exchange recovery of rare earth elements from uranium mining solutions, in: A.A. Rempel, V.A. Volkovich (Eds.) *Physics, Technologies and Innovation* 2016.
- [28] X. Hères, V. Blet, P. Di Natale, A. Ouattou, H. Mazouz, D. Dhiba, F. Cuer, Selective extraction of rare earth elements from phosphoric acid by ion exchange resins, *Metals* 8 (2018) 682.
- [29] F.J. Alguacil, I. Garcia-Diaz, E.E. Baquero, O.R. Largo, F.A. Lopez, On the adsorption of cerium(III) using multiwalled carbon nanotubes, *Metals* 10 (2020) 1057.
- [30] L. Alcaraz, D.N. Saquina, F.J. Alguacil, E. Escudero, F.A. Lopez, Application of activated carbon obtained from spent coffee ground wastes to effective terbium recovery from liquid solutions, *Metals* 11 (2021) 630.
- [31] J. Guo, J. Cai, Q. Su, Ion imprinted polymer particles of neodymium: synthesis, characterization and selective recognition, *J. Rare Earths* 27 (2009) 22–27.
- [32] W.C. Wilfong, T. Ji, Y.H. Duan, F. Shi, Q.M. Wang, M.L. Gray, Critical review of functionalized silica sorbent strategies for selective extraction of rare earth elements from acid mine drainage, *J. Hazard. Mater.* 424 (2022).
- [33] E.C. Giese, Biosorption as green technology for the recovery and separation of rare earth elements, *World J. Microbiol. Biotechnol.* 36 (2020) 52.
- [34] S. Rangabhashiyam, K. Vijayaraghavan, Biosorption of Tm(III) by free and polysulfone-immobilized *Turbinaria conoides* biomass, *J. Ind. Eng. Chem.* 80 (2019) 318–324.
- [35] M.F. Hamza, K.A.M. Salih, A.A.H. Abdel-Rahman, Y.E. Zayed, Y. Wei, J. Liang, E. Guibal, Sulfonic-functionalized algal/PEI beads for scandium, cerium and holmium sorption from aqueous solutions (synthetic and industrial samples), *Chem. Eng. J.* 403 (2021) 126399.
- [36] H.-J. Park, L.L. Tavlarides, Adsorption of neodymium(III) from aqueous solutions using a phosphorus functionalized adsorbent, *Ind. Eng. Chem. Res.* 49 (2010) 12567–12575.
- [37] D.L. Ramasamy, V. Puhakka, S. Iftikhar, A. Wojtus, E. Repo, S. Ben Hammouda, E. Iakovleva, M. Sillanpää, N- and O- ligand doped mesoporous silica-chitosan hybrid beads for the efficient, sustainable and selective recovery of rare earth elements (REE) from acid mine drainage (AMD): understanding the significance of physical modification and conditioning of the polymer, *J. Hazard. Mater.* 348 (2018) 84–91.
- [38] R.G. Pearson, *Acids and bases*, Science 151 (1966) 172–177.
- [39] E. Nieboer, D.H.S. Richardson, The replacement of the non-descript term heavy-metals by a biologically and chemically significant classification of metal-ions, *Environ. Pollut. Ser. B* 1 (1980) 3–26.
- [40] S.D. Alexandratos, S. Natesan, Ion-selective polymer-supported reagents: the principle of bifunctionality, *Eur. Polym. J.* 35 (1999) 431–436.
- [41] S.D. Alexandratos, S.D. Smith, Intraligand cooperation in metal-ion binding by immobilized ligands: the effect of bifunctionality, *J. Appl. Polym. Sci.* 91 (2004) 463–468.
- [42] O. Dudarko, N. Kobylinska, B. Mishra, V.G. Kessler, B.P. Tripathi, G. A. Seisenbaeva, Facile strategies for synthesis of functionalized mesoporous silicas for the removal of rare-earth elements and heavy metals from aqueous systems, *Microporous Mesoporous Mater.* 315 (2021).
- [43] W. Tang, X. Zhang, New chiral phosphorus ligands for enantioselective hydrogenation, *Chem. Rev.* 103 (2003) 3029–3070.
- [44] H. Fernández-Pérez, P. Etayo, A. Panossian, A. Vidal-Ferran, Phosphine–phosphinite and phosphine–phosphite ligands: preparation and applications in asymmetric catalysis, *Chem. Rev.* 111 (2011) 2119–2176.
- [45] S. Kuang, Z. Zhang, Y. Li, G. Wu, H. Wei, W. Liao, Selective extraction and separation of Ce(IV) from thorium and trivalent rare earths in sulfate medium by an alpha-aminophosphonate extractant, *Hydrometallurgy* 167 (2017) 107–114.
- [46] S. Kuang, W. Liao, Progress in the extraction and separation of rare earths and related metals with novel extractants: A review, *Sci. China Technol. Sci.* 61 (2018) 1319–1328.
- [47] S.D. Alexandratos, X. Zhu, M. Florent, R. Sellin, Polymer-supported bifunctional amidoximes for the sorption of uranium from seawater, *Ind. Eng. Chem. Res.* 55 (2016) 4208–4216.
- [48] J. Muller, B. Prelot, J. Zajac, S. Monge, Synthesis and study of sorption properties of polyvinyl alcohol (PVA)-based hybrid materials, *React. Funct. Polym.* 144 (2019).
- [49] Y. Zhou, Y. Gao, H. Wang, M. Xia, Q. Yue, Z. Xue, J. Zhu, J. Yu, W. Yin, Versatile 3D reduced graphene oxide/poly(amino-phosphonic acid) aerogel derived from waste acrylic fibers as an efficient adsorbent for water purification, *Sci. Total Environ.* 776 (2021) 145973.
- [50] S. Iftikhar, V. Srivastava, M. Sillanpää, Synthesis and application of LDH intercalated cellulose nanocomposite for separation of rare earth elements (REEs), *Chem. Eng. J.* 309 (2017) 130–139.
- [51] E.A. Imam, I. El-Tantawy El-Sayed, M.G. Mahfouz, A.A. Tolba, T. Akashi, A. A. Galhoum, E. Guibal, Synthesis of α -aminophosphonate functionalized chitosan sorbents: effect of methyl vs phenyl group on uranium sorption, *Chem. Eng. J.* 352 (2018) 1022–1034.
- [52] R.R. Neiber, A.A. Galhoum, I. El-Tantawy El-Sayed, E. Guibal, J. Xin, X. Lu, Selective lead (II) sorption using aminophosphonate-based sorbents: effect of amine linker, characterization and sorption performance, *Chem. Eng. J.* 442 (2022) 136300.
- [53] M.M. Rashad, I.E. El-Sayed, A.A. Galhoum, M.M. Abdeen, H.I. Mira, E.A. Elshehy, S. Zhang, X. Lu, J. Xin, E. Guibal, Synthesis of α -aminophosphonate based sorbents – Influence of inserted groups (carboxylic vs. amine) on uranyl sorption, *Chem. Eng. J.* 421 (2021) 127830.
- [54] E.A. Imam, A.I. Hashem, A.A. Tolba, M.G. Mahfouz, I.E.-T. El-Sayed, A.I. El-Tantawy, A.A. Galhoum, E. Guibal, Effect of mono- vs. bi-functionality of aminophosphonate derivatives on the enhancement of U(VI) sorption: physicochemical properties and sorption performance, *J. Environ. Chem. Eng.* 11 (2023) 109951.
- [55] O. Falyouna, O. Eljamal, I. Maamoun, A. Tahara, Y. Sugihara, Magnetic zeolite synthesis for efficient removal of cesium in a lab-scale continuous treatment system, *J. Colloid Interface Sci.* 571 (2020) 66–79.
- [56] A.M. Abdel-Rehim, An innovative method for processing Egyptian monazite, *Hydrometallurgy* 67 (2002) 9–17.
- [57] A. Sroor, Passive and active measurements of Egyptian monazite samples, *Appl. Radiat. Isot.* 58 (2003) 281–285.
- [58] O.A. Desouky, A.M. Daher, Y.K. Abdel-Monem, A.A. Galhoum, Liquid-liquid extraction of yttrium using primene-JMT from acidic sulfate solutions, *Hydrometallurgy* 96 (2009) 313–317.
- [59] C.K. Gupta, N. Krishnamurthy, *Extractive Metallurgy of Rare Earths*, CRC Press, Boca Raton (FL), USA, 2005, 2005.
- [60] C. Morais, J. Benedetto, V. Ciminelli, Recovery of cerium by oxidation/hydrolysis with $\text{KMnO}_4\text{-Na}_2\text{CO}_3$, in: C.A. Young, A.M. Alfantazani, C.G. Anderson, D. B. Dreisinger, B. Harris, A. James (Eds.), *Hydrometallurgy 2003 - Fifth International Conference in Honor of professor Ian Ritchie*, TMS, The Minerals, Metals & Materials Society, 2003, pp. 1773–1782.
- [61] S. Omwoma Lugasi, New Synthetic pathways for thiocarbonylazide and salicylaldehyde azine compounds, *Asian J. Chem. Sci.* 3 (2017) 1–8.
- [62] D.P. Singh, R. Kumar, V. Malik, P. Tyagi, Template synthesis, spectroscopic studies and analytical activities of macrocyclic complexes derived from thiocarbonylazide and glyoxal, *J. Enzym. Inhib. Med. Chem.* 22 (2007) 177–182.
- [63] J.R. Mohrig, C.N. Hammond, P.F. Schatz, *Infrared spectroscopy in techniques in organic chemistry*, 2006.
- [64] B.C. Smith, Organic nitrogen compounds II: primary amines, *Spectroscopy* 34 (2019) 22–25.
- [65] L.F. Zhang, G. Liu, Y.G. Wang, J. Shen, R.F. Li, J.K. Du, Z.F. Yang, Q.B. Xu, Modification of coal tar pitch with p-phthalaldehyde to reduce toxic PAH content, *Energy Sources Part A* 38 (2016) 737–743.
- [66] A.M. Borreguero, M.M. Velencoso, J.F. Rodríguez, Á. Serrano, M.J. Carrero, M. J. Ramos, Synthesis of aminophosphonate polyols and polyurethane foams with improved fire retardant properties, *Appl. Polym. Sci.* 136 (2019) 47780.
- [67] M.C. Zenobi, C.V. Luengo, M.J. Avena, E.H. Rueda, An ATR-FTIR study of different phosphonic acids adsorbed onto boehmite, *Spectrochim. Acta, Part A* 75 (2010) 1283–1288.
- [68] K.A. Elachi, S. Hossain, M.M. Haque, R.K. Mohapatra, K. E-Zahan, Synthesis, spectral and thermal characterization of Cu(II) complexes containing Schiff base ligands and their antibacterial activity study, *Am. J. Mater. Synth. Process.* 4 (2019) 43–53.
- [69] C. He, K.A.M. Salih, Y. Wei, H. Mira, A.A.H. Abdel-Rahman, K.Z. Elwakeel, M. F. Hamza, E. Guibal, Efficient recovery of rare earth elements (Pr(III) and Tm(III)) from mining residues using a new phosphorylated hydrogel (algal biomass/PEI), *Metals* (2021) 294.
- [70] A.A. Galhoum, E.A. Elshehy, D.A. Tolan, A.M. El-Nahas, T. Taketsugu, K. Nishikiori, T. Akashi, A.S. Morshedy, E. Guibal, Synthesis of polyaminophosphonic acid-functionalized poly(glycidyl methacrylate) for the efficient sorption of La(III) and Y(III), *Chem. Eng. J.* 375 (2019) 121932.
- [71] A. Fernandez-Botello, R.B. Gomez-Coca, A. Holy, V. Moreno, H. Sigel, Metal-ion binding properties of O-phosphonatomethylcholine (PMCh(-)). Effect of the

- positive charge of a distant trimethylammonium group on the coordinating qualities of a phosph(on)ate group, *Inorg. Chim. Acta* 331 (2002) 109–116.
- [72] S.D. Alexandratos, X. Zhu, Immobilized tris(hydroxymethyl)aminomethane as a scaffold for ion-selective ligands: the auxiliary group effect on metal ion binding at the phosphate ligand, *Inorg. Chem.* 46 (2007) 2139–2147.
- [73] W. Zhang, S. Yu, S. Zhang, J. Zhou, S. Ning, X. Wang, Y. Wei, Separation of scandium from the other rare earth elements with a novel macro-porous silica-polymer based adsorbent HDEHP/SiO₂-P, *Hydrometallurgy* 185 (2019) 117–124.
- [74] W. Zhang, D. Feng, X. Xie, X. Tong, Y. Du, Y. Cao, Solvent extraction and separation of light rare earths from chloride media using HDEHP-P350 system, *J. Rare Earths* 40 (2022) 328–337.
- [75] Y. Xiong, W. Kuang, J. Zhao, H. Liu, Ionic liquid-based synergistic extraction of rare earths nitrates without diluent: typical ion-association mechanism, *Sep. Purif. Technol.* 179 (2017) 349–356.
- [76] K. Burdzy, A. Aurich, S. Hunger, R. Jastrzab, M. Zabiszak, D. Kolodynska, Green citric acid in the sorption process of rare earth elements, *Chem. Eng. J.* 437 (2022).
- [77] J.E. Quinn, K.H. Soldenhoff, G.W. Stevens, Solvent extraction of rare earth elements using a bifunctional ionic liquid. Part 2: Separation of rare earth elements, *Hydrometallurgy* 169 (2017) 621–628.
- [78] K. Huang, Y. Jia, S. Wang, J. Yang, H. Zhong, A novel method for synthesis of styryl phosphonate monoester and its application in La(III) extraction, *J. Rare Earths* 38 (2020) 649–656.
- [79] E.J. Virtanen, S. Perämäki, K. Helttunen, A. Väisänen, J.O. Moilanen, Alkyl-substituted aminobis(phosphonates)—Efficient precipitating agents for rare earth elements, thorium, and uranium in aqueous solutions, *ACS Omega* 6 (2021) 23977–23987.
- [80] M. Weller, T. Overton, J. Rourke, F. Armstrong (Oxford University Press.). *Inorganic Chemistry*, sixth ed., Oxford University Press, 2014.
- [81] D. Kolodynska, J. Bak, M. Majdanska, D. Fila, Sorption of lanthanide ions on biochar composites, *J. Rare Earths* 36 (2018) 1212–1220.
- [82] J. Crank. *The Mathematics of Diffusion*, second. ed., Oxford University Press., Oxford, U.K., 1975.
- [83] A.A. Naser, G.E.S. El-Deen, A.A. Bhran, S.S. Metwally, A.M. El-Kamash, Elaboration of impregnated composite for sorption of europium and neodymium ions from aqueous solutions, *J. Ind. Eng. Chem.* 32 (2015) 264–272.
- [84] D. Fila, Z. Hubicki, D. Kolodynska, Applicability of new sustainable and efficient alginate-based composites for critical raw materials recovery: General composites fabrication optimization and adsorption performance evaluation, *Chem. Eng. J.* 446 (2022) 137245.
- [85] Y. Marcus, *Ion Properties*, Marcel Dekker, Inc., New York, NY, 1997.
- [86] C. Tien, *Adsorption calculations and modeling*. Butterworth-Heinemann, Butterworth-Heinemann, Boston, 1994.
- [87] S. Kalam, S.A. Abu-Khamsin, M.S. Kamal, S. Patil, Surfactant adsorption isotherms: a review, *ACS Omega* 6 (2021) 32342–32348.
- [88] V. Puccia, M.J. Avena, On the use of the Dubinin-Radushkevich equation to distinguish between physical and chemical adsorption at the solid-water interface, *Colloid Interface Sci. Commun.* 41 (2021) 100376.
- [89] H.N. Tran, E.C. Lima, R.-S. Juang, J.-C. Bollinger, H.-P. Chao, Thermodynamic parameters of liquid-phase adsorption process calculated from different equilibrium constants related to adsorption isotherms: a comparison study, *J. Environ. Chem. Eng.* 9 (2021) 106674.
- [90] A.I. Abd-Elhamid, E.M. Abu Elgoud, H.F. Aly, Graphene oxide modified with carboxymethyl cellulose for high adsorption capacities towards Nd(III) and Ce (III) from aqueous solutions, *Cellulose* 29 (2022) 9831–9846.
- [91] M.F. Hamza, A.A.H. Abdel-Rahman, E. Guibal, Magnetic glutamine-grafted polymer for the sorption of U(VI), Nd(III) and Dy(III), *J. Chem. Technol. Biotechnol.* 93 (2018) 1790–1806.
- [92] Y. Wei, K.A.M. Salih, K. Rabie, K.Z. Elwakeel, Y.E. Zayed, M.F. Hamza, E. Guibal, Development of phosphoryl-functionalized algal-PEI beads for the sorption of Nd (III) and Mo(VI) from aqueous solutions ? Application for rare earth recovery from acid leachates, *Chem. Eng. J.* 412 (2021).
- [93] H. Demey, B. Lapo, M. Ruiz, A. Fortuny, M. Marchand, A.M. Sastre, Neodymium recovery by chitosan/iron(III) hydroxide ChiFer(III) sorbent material: Batch and column systems, *Polymers* 10 (2018).
- [94] Y. Konishi, S. Asai, J. Shimaoka, M. Miyata, T. Kawamura, Recovery of neodymium and ytterbium by biopolymer gel particles of alginic acid, *Ind. Eng. Chem. Res.* 31 (1992) 2303–2311.
- [95] R.C. Oliveira, E. Guibal, O. Garcia Jr., Biosorption and desorption of lanthanum (III) and neodymium(III) in fixed-bed columns with *Sargassum sp.*: Perspectives for separation of rare earth metals, *Biotechnol. Progr.* 28 (2012) 715–722.
- [96] L. Zhang, D. Wu, B. Zhu, Y. Yang, L. Wang, Adsorption and selective separation of neodymium with magnetic alginate microcapsules containing the extractant 2-ethylhexyl phosphonic acid mono-2-ethylhexyl ester, *J. Chem. Eng. Data* 56 (2011) 2280–2289.
- [97] J. Roosen, J. Pype, K. Binnemans, S. Mullens, Shaping of alginate-silica hybrid materials into microspheres through vibrating-nozzle technology and their use for the recovery of neodymium from aqueous solutions, *Ind. Eng. Chem. Res.* 54 (2015) 12836–12846.
- [98] W.R. Mohamed, S.S. Metwally, H.A. Ibrahim, E.A. El-Sherief, H.S. Mekhamer, I. M.I. Moustafa, E.M. Mabrouk, Impregnation of task-specific ionic liquid into a solid support for removal of neodymium and gadolinium ions from aqueous solution, *J. Mol. Liq.* 236 (2017) 9–17.
- [99] A.A. Galhoum, T. Akashi, M. Linnolahti, J.T. Hirvi, A.G. Al-Sehemi, A. Kalam, E. Guibal, Functionalization of poly(glycidylmethacrylate) with iminodiacetate and imino phosphonate groups for enhanced sorption of neodymium-sorption performance and molecular modeling, *React. Funct. Polym.* 180 (2022).
- [100] L.S. Ismail, F.I. Khalili, Biosorption of neodymium(III) and cerium(III) ions by Loquat leaves (*Eriobotrya japonica*) kinetics and thermodynamic studies, *Desalin. Water Treat.* 229 (2021) 291–301.
- [101] Gd.V. Brião, M.G.C. da Silva, M.G.A. Vieira, Efficient and selective adsorption of neodymium on expanded vermiculite, *Ind. Eng. Chem. Res.* 60 (2021) 4962–4974.
- [102] Gd.V. Brião, M.G.Cd Silva, M.G.A. Vieira, Neodymium recovery from aqueous solution through adsorption/desorption onto expanded vermiculite, *Appl. Clay Sci.* 198 (2020) 105825.
- [103] S. Kinoshita, N. Koizumi, M. Ueno, N. Okumura, K. Imai, H. Tanaka, Y. Yamamoto, T. Nakamura, T. Inatomi, J. Bush, M. Toda, M. Hagiya, I. Yokota, S. Teramukai, C. Sotozono, J. Hamuro, Injection of cultured cells with a ROCK inhibitor for bullous keratopathy, *N. Engl. J. Med.* 378 (2018) 995–1003.
- [104] R.A. Plessl K, D. Vollprecht, Application and development of zero-valent iron (ZVI) for groundwater and wastewater treatment, *Int. J. Environ. Sci. Technol.* 10 (2023) 6913–6928.
- [105] K. Li, M. Li, D. Xue, Solution-phase electronegativity scale: Insight into the chemical behaviors of metal ions in solution, *J. Phys. Chem. A* 116 (2012) 4192–4198.
- [106] S. Ravi, P. Puthiaraj, K. Yu, W.S. Ahn, Porous covalent organic polymers comprising a phosphite skeleton for aqueous Nd(III) capture, *ACS Appl. Mater. Interfaces* 11 (2019) 11488–11497.
- [107] I. Persson, Hydrated metal ions in aqueous solution: How regular are their structures, *Pure Appl. Chem.* 82 (2010) 1901–1917.
- [108] A. Vlachou, B.D. Symeopoulos, A.A. Koutinas, A comparative study of neodymium sorption by yeast cells, *Radiochim. Acta* 97 (2009) 437–441.
- [109] A.R. Elsalamouny, O.A. Desouky, S.A. Mohamed, A.A. Galhoum, E. Guibal, Uranium and neodymium biosorption using novel chelating polysaccharide, *Int. J. Biol. Macromol.* 104 (2017) 963–968.
- [110] M.A. Kucuker, N. Wiecezorek, K. Kuchta, N.K. Copty, Biosorption of neodymium on *Chlorella vulgaris* in aqueous solution obtained from hard disk drive magnets, *PLoS One* 12 (2017) e0175255.
- [111] M. Khalil, Y.F. El-Aryan, E.M. El, Afifi, Sorption performance of light rare earth elements using zirconium titanate and polyacrylonitrile zirconium titanate ion exchangers, *Part. Sci. Technol.* 36 (2018) 618–627.
- [112] O. Perea, K. Laatikainen, C. Bode-Aluko, O. Fatoba, E. Omoniyi, Y. Kochnev, A. N. Nechaev, P. Apel, L. Petrik, Synthesis and characterisation of diglycolic acid functionalised polyethylene terephthalate nanofibers for rare earth elements recovery, *J. Environ. Chem. Eng.* 9 (2021).
- [113] V. Gutsanu, G. Lisa, D. Rusu, Adsorption of lanthanide(III) cations on cross-linked ionic polymer, composition and thermal analysis of the formed composites, *Colloid J.* 83 (2021) 688–697.
- [114] S. Mahajan, V. Srivastava, M. Sillanpaa, Novel poly-D-galacturonic acid methyl ester grafted vinyl monomer polymer super green adsorbent via C-O strategic protrusion of methyl methacrylate (MMA) for removal of Sm (III) and Nd (III), *Sep. Purif. Technol.* 258 (2021).
- [115] Q. Zhao, Y. Wang, Z. Xu, Z. Yu, The potential use of straw-derived biochar as the adsorbent for La(III) and Nd(III) removal in aqueous solutions, *Environ. Sci. Pollut. Res.* 28 (2021) 47024–47034.
- [116] Y. El Ouardi, M. Lamsayah, S. Butylina, S. Geng, M. Esmaeli, A. Giove, E.S. M. Mouele, S. Virolainen, S. El Barkany, A. Ouammou, E. Repo, K. Laatikainen, Sustainable composite material based on glutenin biopolymeric-clay for efficient separation of rare earth elements, *Chem. Eng. J.* 440 (2022).
- [117] A. Vardanyan, A. Guillon, T. Budnyak, G.A. Seisenbaeva, Tailoring nano-adsorbent surfaces: separation of rare earths and late transition metals in recycling of magnet materials, *Nanomaterials* 12 (2022) 974.
- [118] F.-Y. Huang, Z. Wang, F.-C. Yi, Y. Liu, Y.-D. Wu, Y. Luo, W.-J. Jia, Sorption behavior and mechanism of simulated radionuclide Nd(III) from aqueous solution by bentonite, *Russ. J. Phys. Chem. A* 96 (2022) 1077–1084.